Fe-based superconductors (FBS) at high magnetic fields

Alex Gurevich

Old Dominion University, Norfolk, VA

Dept. Physics, University of Virginia, Sept. 26, 2011

Outline

- Fe-based superconductors: unconventional multiband superconductivity mediated by magnetic fluctuations

- High T_c and huge upper critical magnetic fields. Interplay of orbital and paramagnetic pairbreaking in multiband SCs and their effect on $H_{c2}(T)$

- Manifestations of the $s^{\pm}$ pairing symmetry in the temperature dependence of $H_{c2}(T)$.

- Strong Pauli pairbreaking in FBS can lead to FFLO.
  Does the $s^{\pm}$ pairing facilitate or inhibit the FFLO instability?

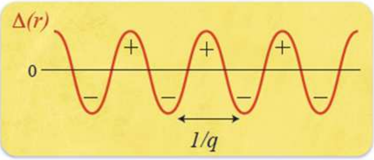

- FFLO in multiband FBS: what happens if one band is FFLO unstable but another one is not?

- Tuning $H_{c2}(T)$ by doping: FFLO triggered by the Lifshitz transition

Diverse family of Fe-based superconductors (FBS)

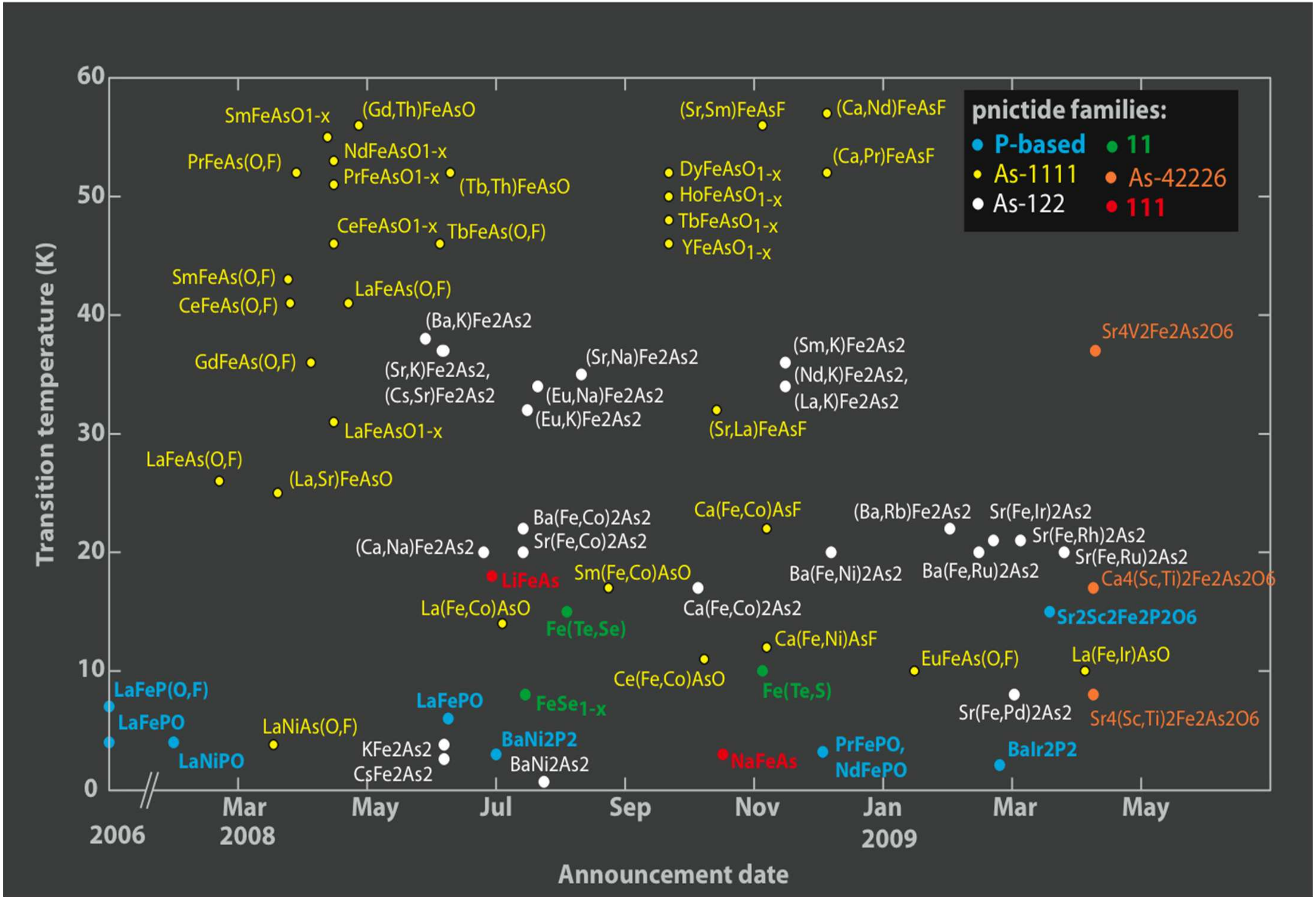

Phenomenology of pnictides

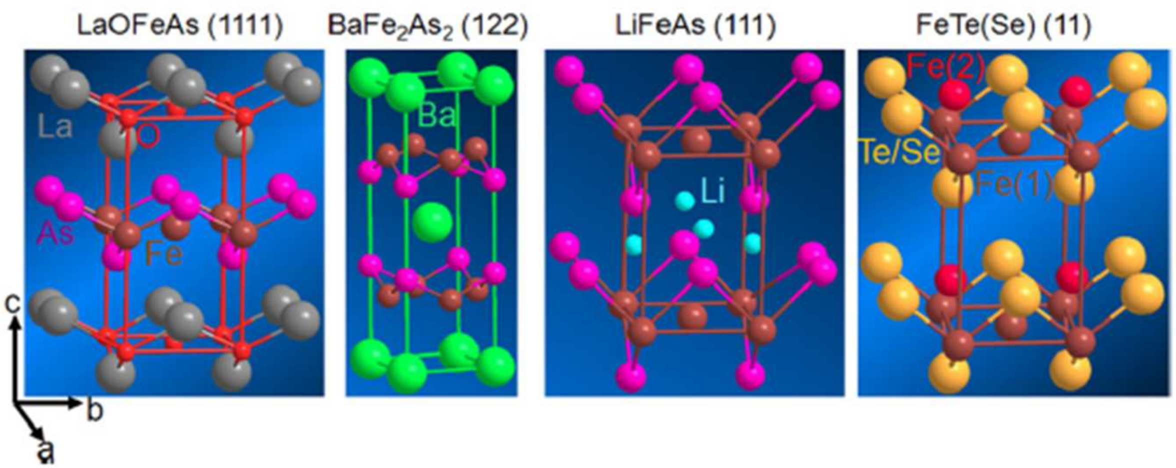

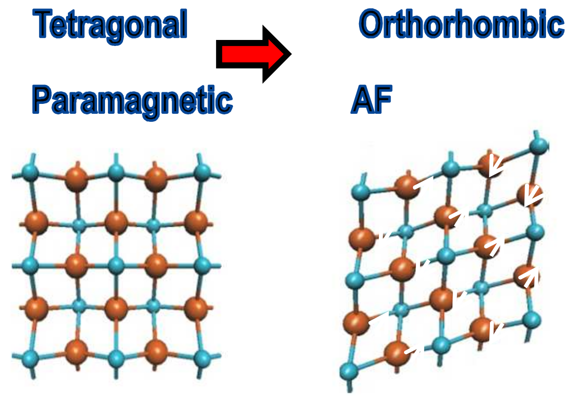

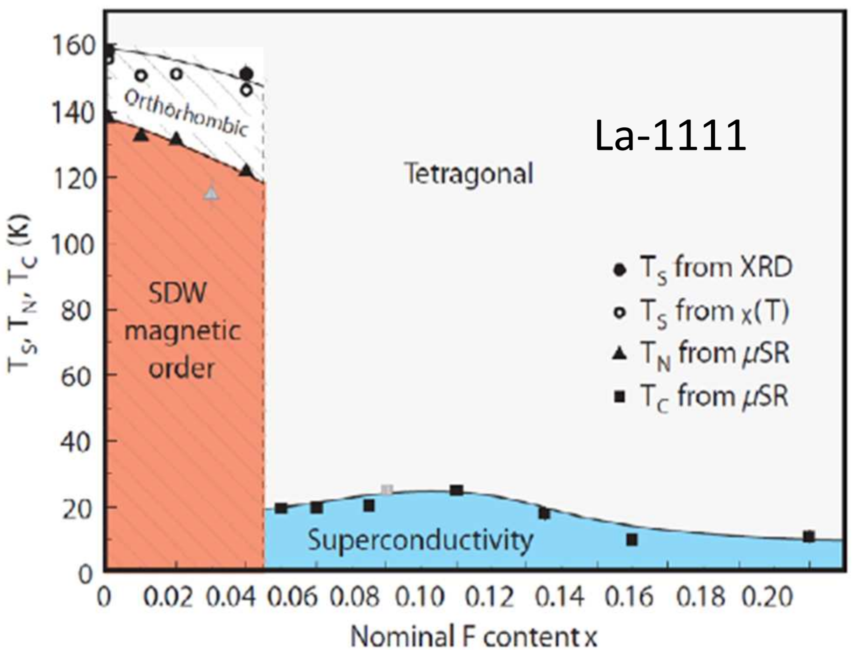

H. Luetkens et al, Nature Mat. 8, 305 (2009)

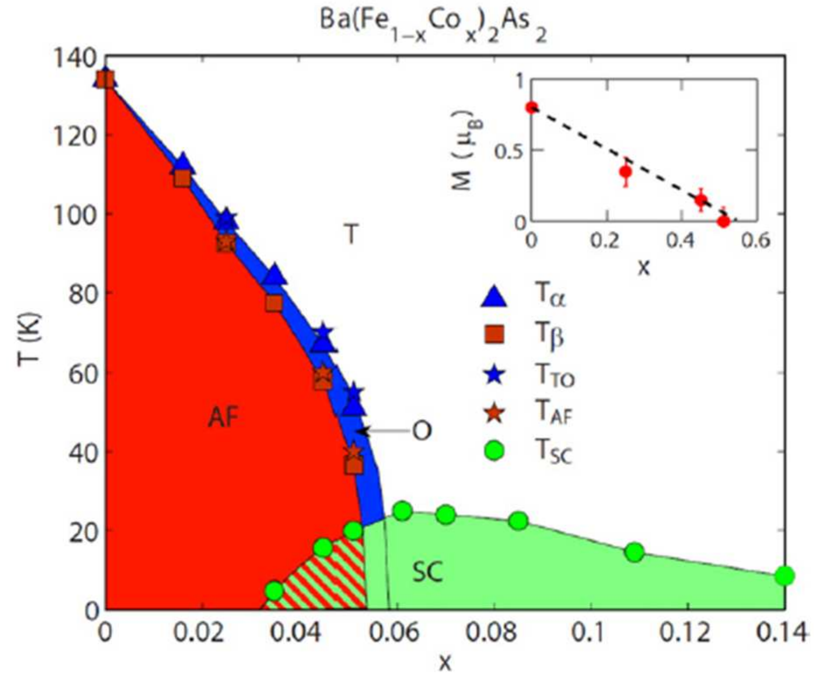

C. Lester et al, PRB 79, 144523 (2009)

Multiband superconductivity in oxypnictides

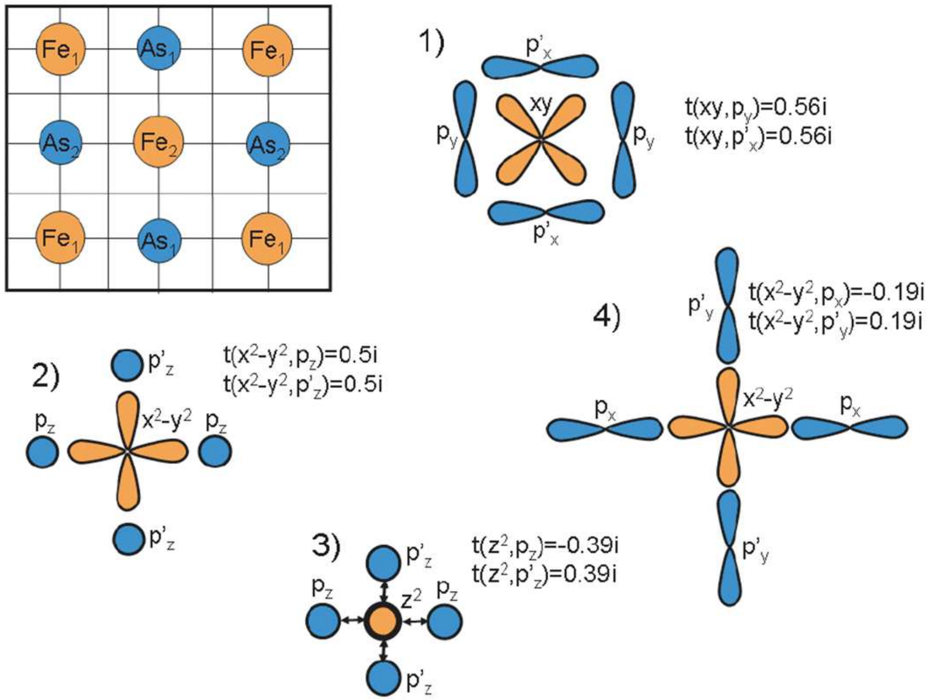

Haule and Kotliar, NJP 025021 (2009)

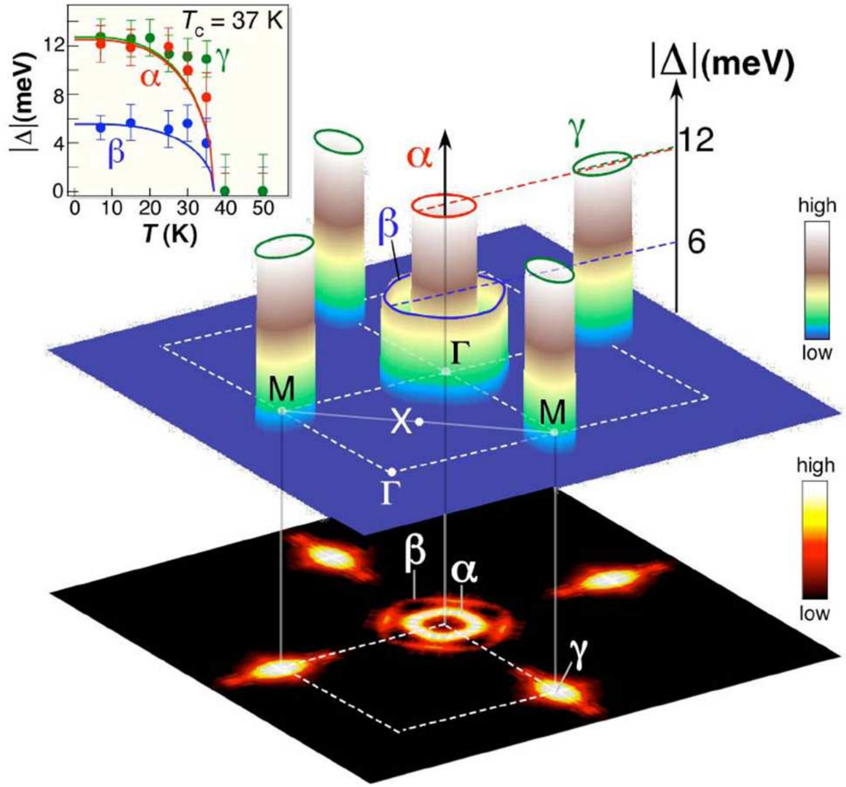

Five d-orbitals of Fe hybridized with p-orbitals of As

Several disconnected pieces of FS

Multiple superconducting gaps

ARPES and tunneling:
$Ba_{0.6}K_{0.4}Fe_2As_2$

Ding et al, EL 83, 47001 (2008)

The Matthias rules are violated:

$$T_c = \Omega e^{-1/NV}$$

- High symmetry is good, cubic symmetry is best
- High density of electronic states is good
- Stay away from oxygen
- Stay away from magnetism
- Stay away from insulators
- Stay away from theorists

Bernd Matthias

Huge H_{c2} in pnictides

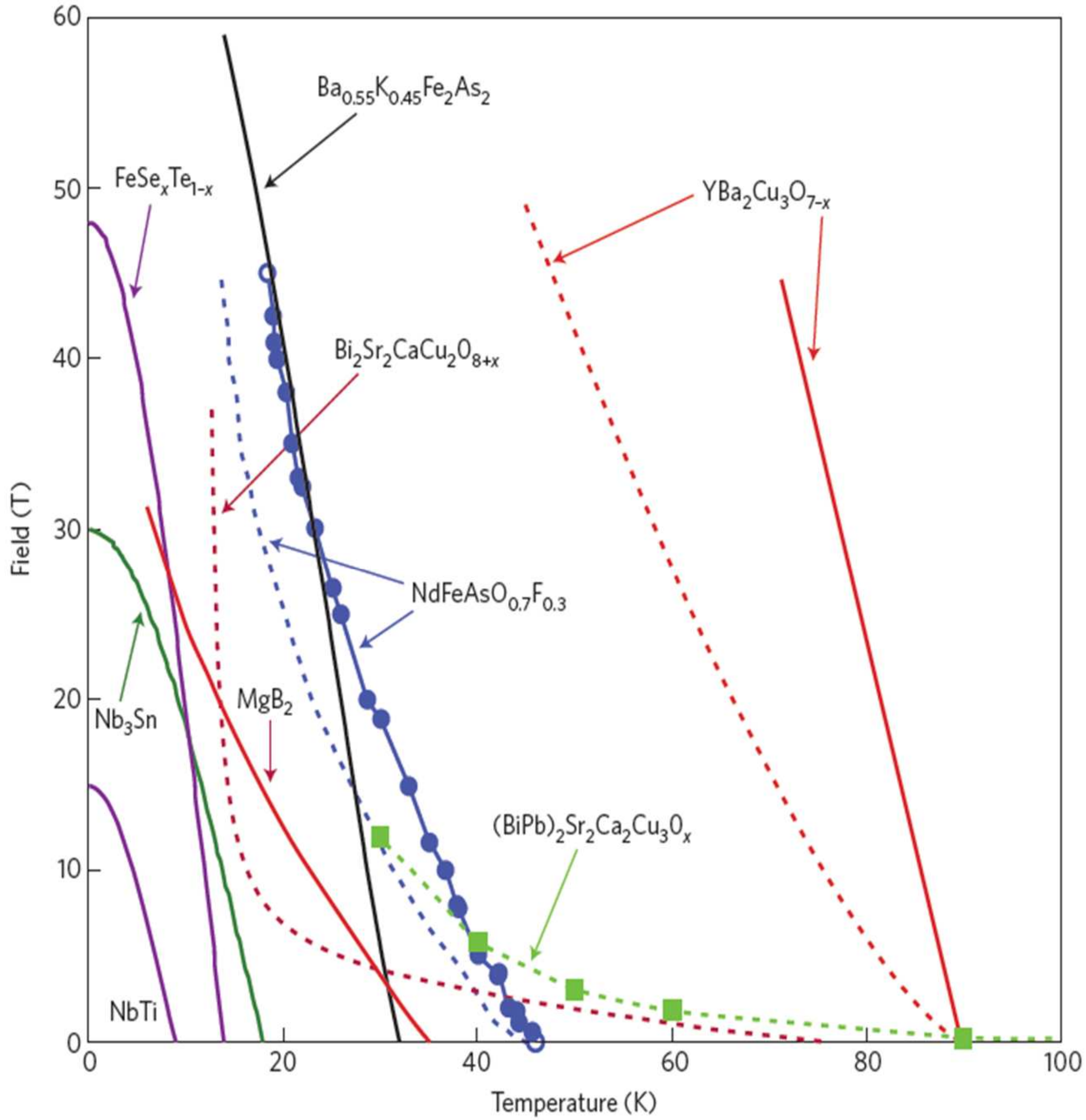

- High slopes H_{c2}' = 2-100 T/K at T_c
- $H_{c2}(0)$ for 1111 and 122 FBS, extrapolate to > 100T
- Short GL coherence lengths

$$\xi_0 = \left[\frac{\phi_0}{2\pi T_c H'_{c2}}\right]^{1/2} = 1-2\ nm$$

result from high T_c and low carrier density in semi-metallic FBS

$$\xi_0 = \frac{\hbar v_F}{2\pi T_c}$$

Dirty limit can hardly be reached

AG, Nature Mat. 10, 255 (2011)

High-field measurements at NHMFL

45T Hybrid Magnet
Highest DC Magnetic Field

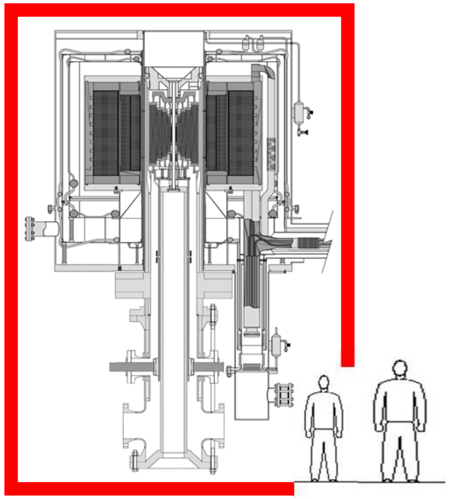

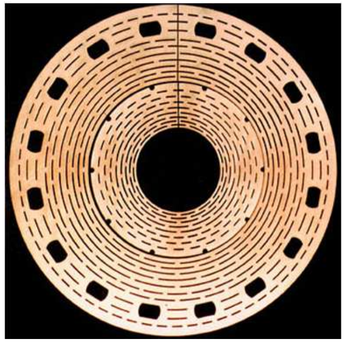

"world's highest steady-field resistive (35 T) and hybrid (45 T) magnets"

200T, 1 microsecond
One pulse per hour

NHMFL/LANL

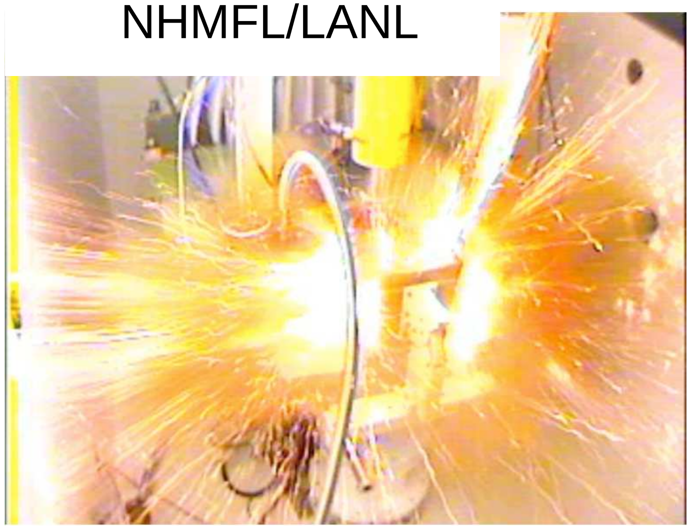

Cooper pairs at high magnetic fields

- Larmor orbital motion of Cooper pairs: Vortex structure and orbital pairbreaking in vortex cores

- Paramagnetic pairbreaking

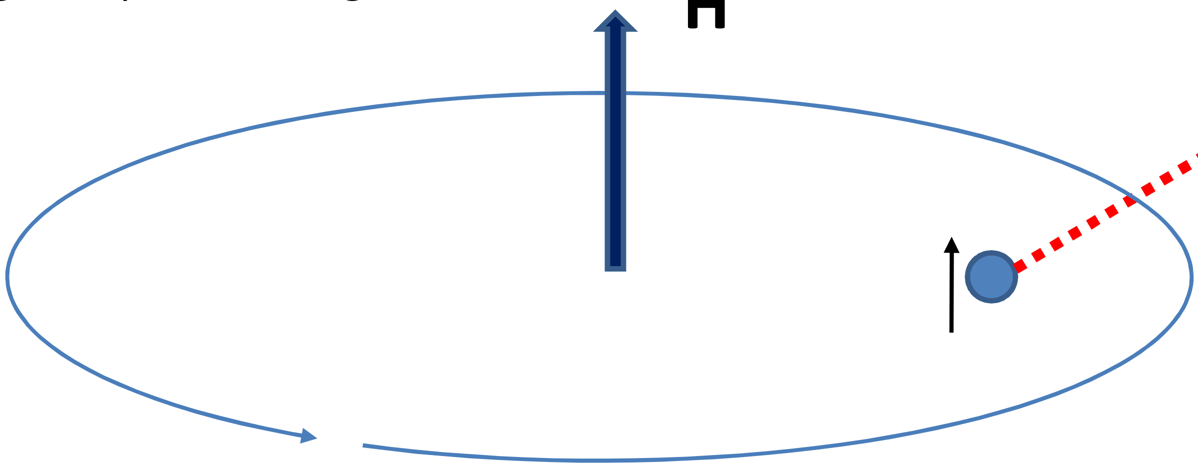

- Critical orbital velocity v_c to destroy superconductivity ⟹ upper critical field: H_{c2}

- Zeeman energy = binding energy of the Cooper pair ⟹ paramagnetic limit: $\mu_B H_p = \Delta$

Type-II superconductors

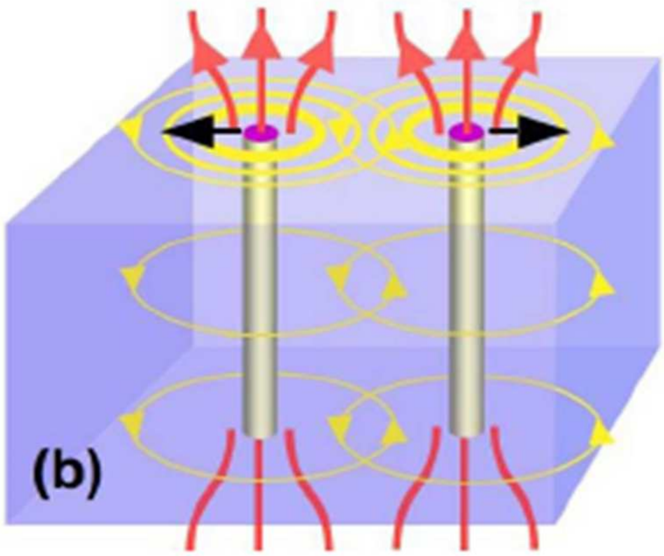

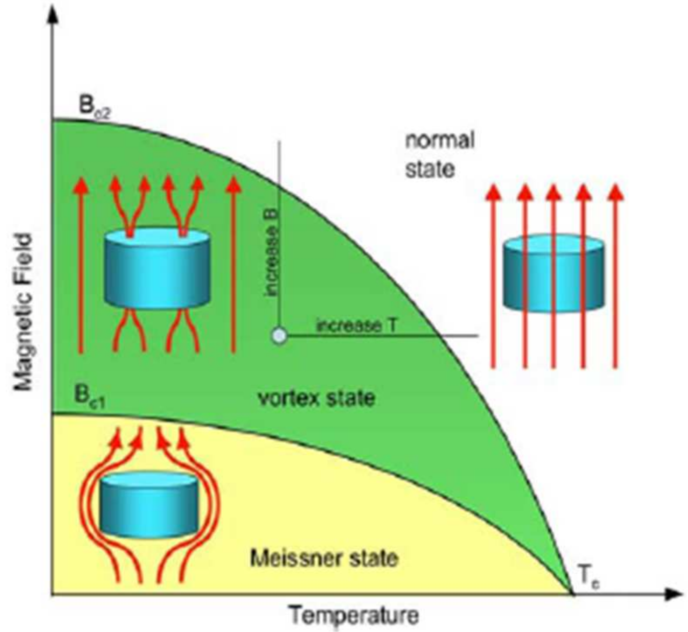

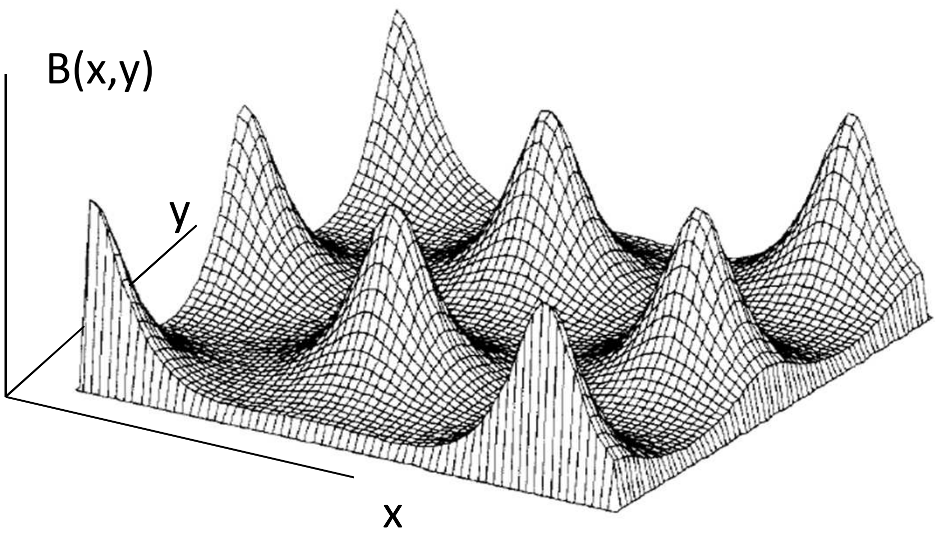

- Hexagonal lattice of vortex lines, each carrying the flux quantum ϕ_0
- Vortex density **$n(B) = \phi_0/B$**
- Spacing between vortices: **$a = (\phi_0/B)^{1/2}$**

Paibreaking velocity, vortex core, and coherence length

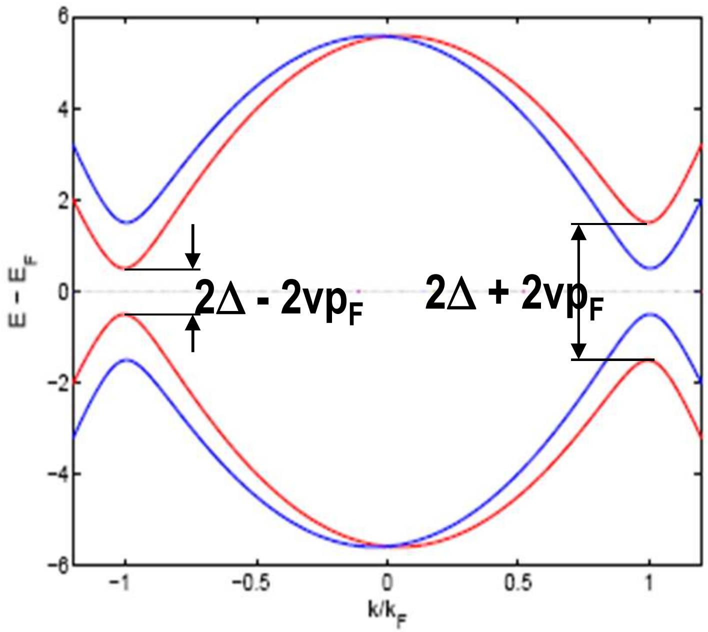

Doppler shift of the electron spectrum in the superflow:

$$E(p) = \pm\sqrt{\Delta^2 + (\varepsilon_p - E_F)^2} \pm \vec{p}_F \vec{v}_s(t)$$

Gap reduction: $\Delta(v_s) = \Delta - p_F|v_s|$ $\Rightarrow$ the critical velocity

$$v_c = \Delta / p_F$$

Superfluid velocity around the vortex and the coherence length ξ:

$$v = \frac{\hbar}{m^* R}, \qquad \frac{\hbar}{m^* \xi} = v_c \quad \Rightarrow \quad \xi = \frac{\hbar v_F}{\Delta}$$

Upper critical field:

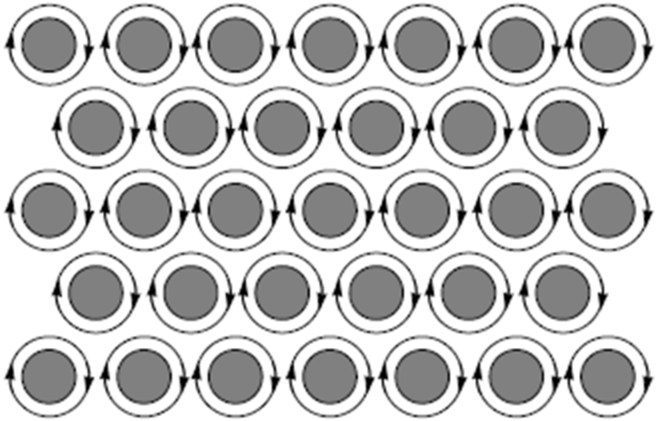

At H = H_{c2} normal vortex cores overlap:

$$(\phi_0 / H)^{1/2} < \xi \quad \Rightarrow \quad H_{c2} = \frac{\phi_0}{2\pi\xi^2}$$

Effect of anisotropy:

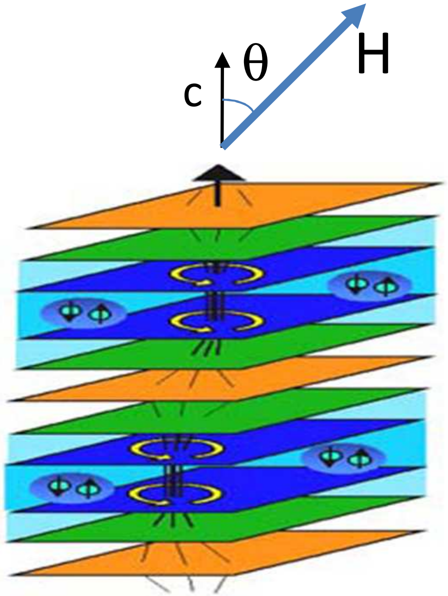

$$H_{c2}(\theta) = \frac{H_{c2}}{\sqrt{\cos^2\theta + \varepsilon \sin^2\theta}}, \qquad \varepsilon = \frac{m_{ab}}{m_c} < 1$$

Enhancement of parallel H_{c2}:

$$H_{c2}^{\parallel} = H_{c2}\sqrt{\frac{m_c}{m_{ab}}} = \frac{\pi^2 c\sqrt{m_{ab} m_c}}{2e\hbar}\frac{\Delta^2}{E_F}$$

Mass anisotropy, high T_c and low E_F greatly enhance H_{c2}

Does increasing H_{c2} by disorder work in FBS?

Effect of the elastic mean free path ℓ on the orbitally-limited $H_{c2} = \phi_0 / 2\pi\xi^2$

(Werhamer-Helfand-Hohenberg, 1966)

Clean limit: $\ell >> \xi_0 \quad \Rightarrow \quad \xi = \xi_0$ and $$H_{c2} \cong \frac{\pi\phi_0\Delta^2}{2\hbar^2 v_F^2} \propto T_c^2$$

Dirty limit : $\ell << \xi_0 \quad \Rightarrow \quad \xi = (\ell\xi_0)^{1/2}$ $$H_{c2} = \frac{\phi_0\Delta}{2\hbar v_F \ell} \propto T_c \rho_n$$

Works in conventional superconductors: 10 –fold increase of H_{c2} in MgB_2

Does not work in FBS because $\ell < \xi_0 \sim$ 1-2 nm implies the Joffe-Regel limit and $\ell k_F < 1$ for which the conventional transport theories fail

H_{c2} in semi-metallic FBS can be effectively tuned by doping

Orbital or Pauli-limited H_{c2}?

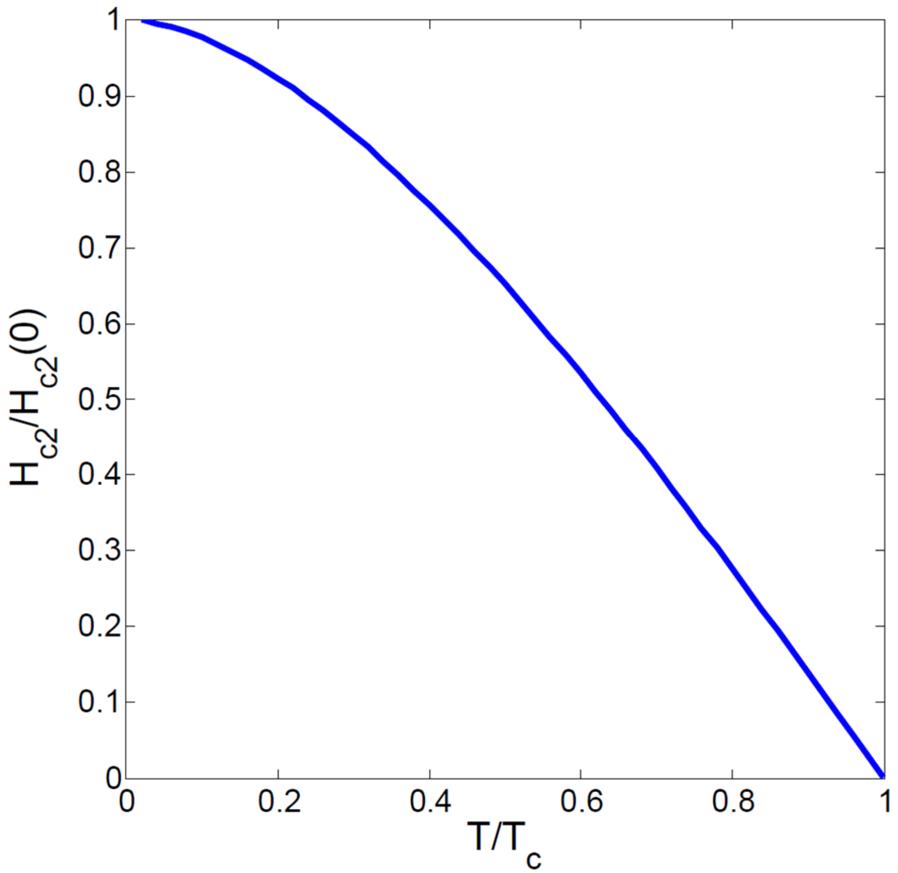

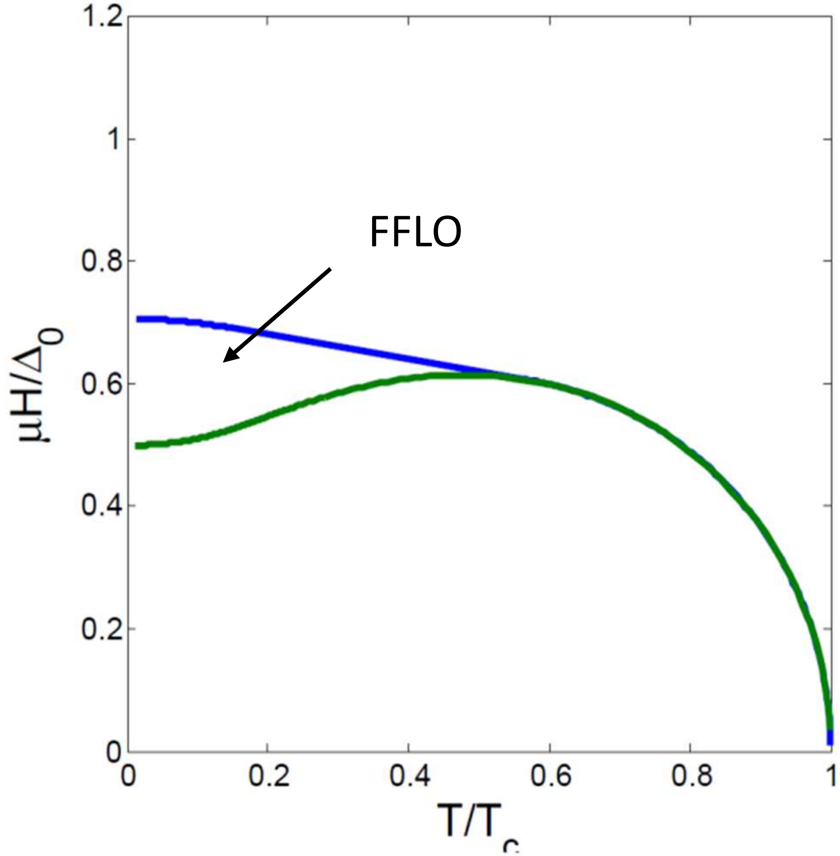

Orbitally limited

Mostly Pauli limited

Werthamer-Helfand-Hohenberg 1963-1965

Sarma, Maki 1963-1964
Gruenberg and Gunther, 1966

Pauli pairbreaking

<u>**Chandrasekhar – Klogston limit**</u>

$$\frac{\chi_n}{2} H_p^2 = N(0)\frac{\Delta^2}{2}, \qquad \chi_n = 2\mu_B^2 N(0)$$

magnetic energy   **condensation energy**

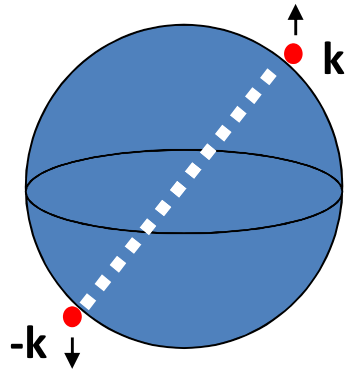

$$\mu_B H_p = \Delta / \sqrt{2}$$

First order phase transition

Using BCS $\Delta = 1.78 k_B T_c$ yields a useful relation

$$H_p[Tesla] = 1.84 T_c[Kelvin]$$

Relation between orbital and Pauli pairbreaking

- Maki parameter **$\alpha_M = 2^{1/2}H_{c2}^{orb}/H_p$:**

$$\alpha_M = \frac{\pi^2\Delta}{4E_F}\frac{m_{ab}}{m_0}, \qquad H \perp ab$$

$$\alpha_M = \frac{\pi^2\Delta}{4E_F}\frac{\sqrt{m_{ab}m_c}}{m_0}, \qquad H \parallel ab$$

- In ordinary metallic BCS superconductors with $m_{ab} \sim m_0$ and $\Delta << E_F$, paramagnetic pairbreaking is negligible , **$\alpha_M << 1$**

Pauli-limited superconductors with $\alpha_M > 1$

- Heavy fermions with **$m_{ab}/m_0 \sim 10^3$**
- Highly anisotropic materials with **$m_c/m_0 \sim 10^6$:** layered organic SC, high-T_c cuprates (BSCCO), etc for **H||ab**
- Semi-metalic, strongly correlated FBS with **$E_F < 0.01\text{-}0.1$ eV**, and **$m_{ab}/m_0 \sim 10$**

Orbital and Pauli coupling: FFLO state

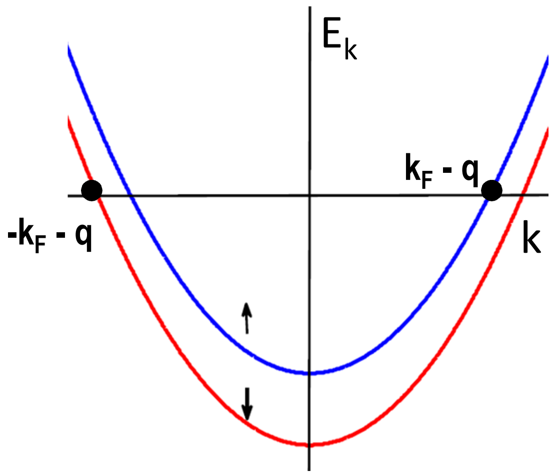

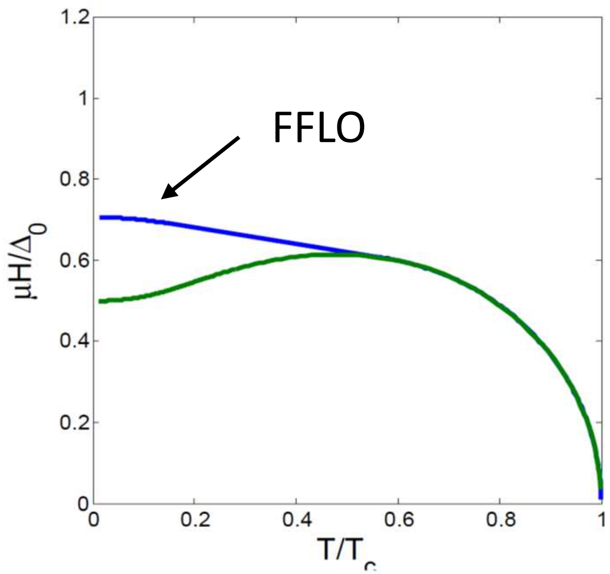

Cooper pairing with nonzero momentum Q = 2q:
modulation of the order parameter along H

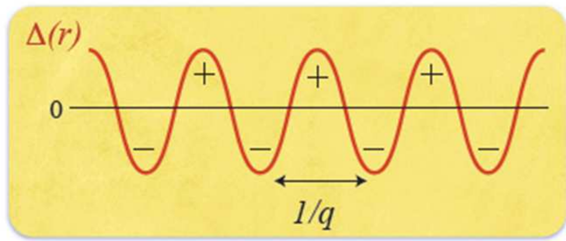

$\Delta(z) = \Delta_0 \cos(Qz)$ (Larkin-Ovchinnikov)
$\Delta(z) = \Delta_0 \exp(iQz)$ (Fulde-Ferrel)

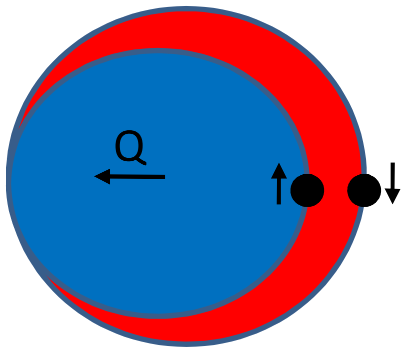

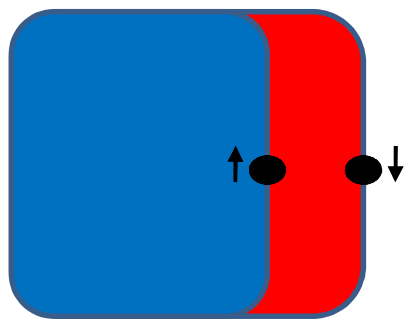

FS nesting facilitates the FFLO state

FFLO in heavy fermions and organics

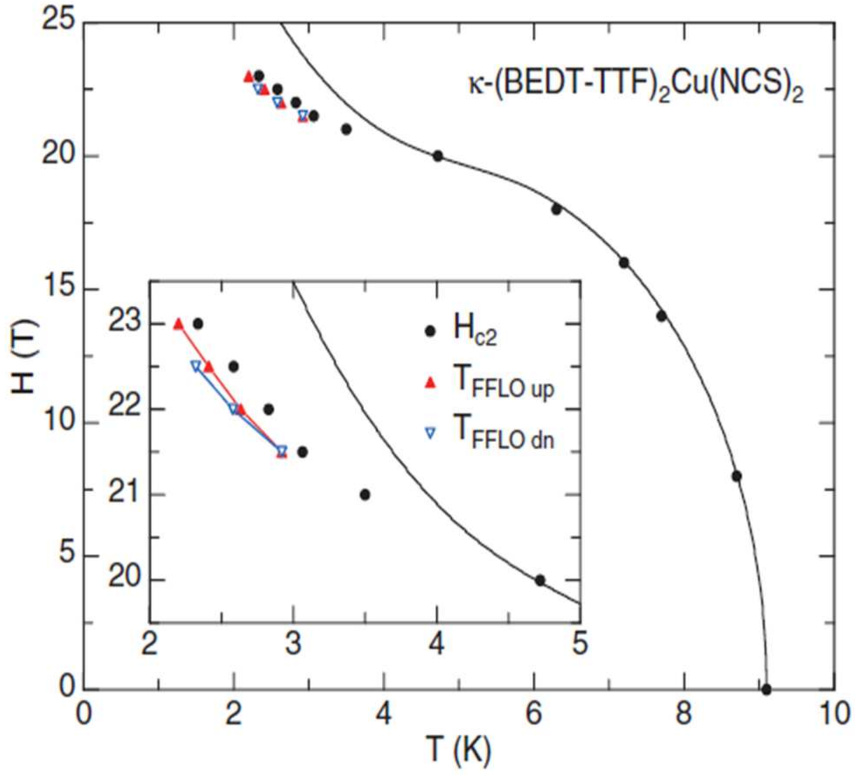

B. Lortz et al, PRL 99, 187002 (2007)

Layered organic SC

$CeCoIn_5$

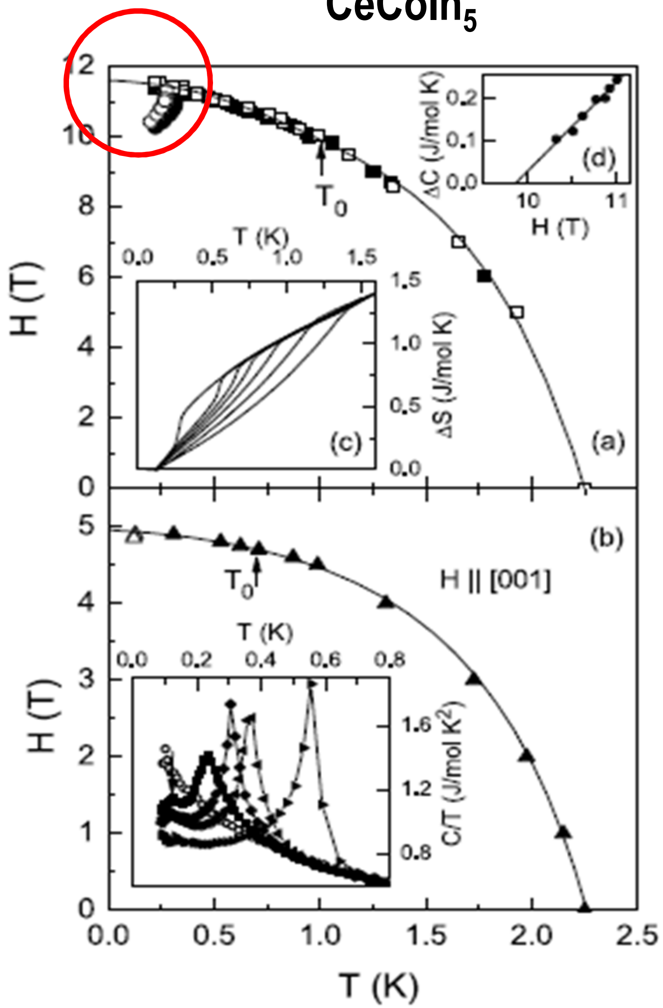

Bianchi et al, PRL 91, 187004 (2003)

Heavy fermions

Theory of anisotropic FFLO (single band)

Linearlized Gor'kov equation in a uniaxial SC with ellipsoidal FS:

$$\Psi(\vec{r}) = \int d^3 r' \Psi(\vec{r}\,') \int D(\vec{k}) \exp\left[i\vec{k}(\vec{r} - \vec{r}\,') + \frac{i\pi}{\phi_0} \vec{H} \cdot (\vec{r} \times \vec{r}\,') \right] \frac{d^3 k}{(2\pi)^3}$$

$$D(k) = \mathrm{Re} \sum_{\omega>0}^{\Omega} \frac{4\pi\lambda T}{v\sqrt{k_\perp^2 + \varepsilon k_z^2}} \tan^{-1} \frac{v\sqrt{k_\perp^2 + \varepsilon k_z^2}}{2(\omega + i\mu_B H)}$$

H_{c2} is an eigenvalue of the Schroedinger equation for a particle with q = 2e
Werthamer and Helfand, (1964)

Tilted first Landau level eigenfunction:

$$\Psi(x, y) = \Delta \exp\left[-\frac{\pi H}{2\phi_0} (c_x x^2 + c_y y^2) \right] \exp[i\vec{Q}\vec{r}]$$

c_x, c_y and the FFLO vector **Q** are determined by the condition that H_{c2} is maximum

Exact solution

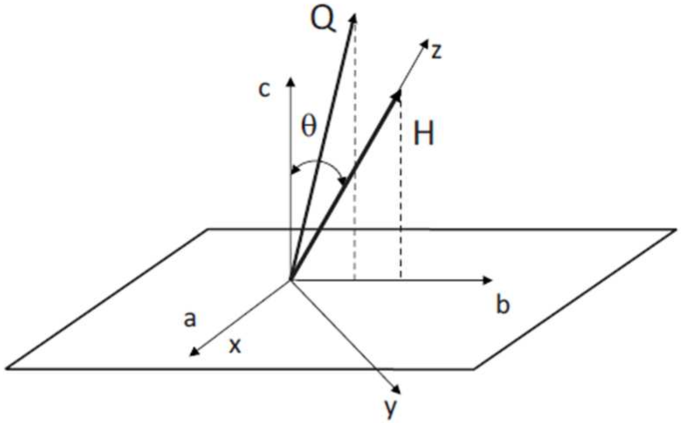

- FFLO wave vector **Q** is not parallel to **H** unless **H** is along the symmetry axis. The angle γ between **Q** and **H**:

$$\tan\gamma = -\frac{(1-\varepsilon)\sin 2\theta}{2(\cos^2\theta + \varepsilon\sin^2\theta)}$$

- Competition between the FFLO kinetic energy εQ_z^2 and the Zeeman energy

- GL angular scaling works for all T
(Brison et al, Physica C 250, 198 (1995))

- H_{c2} is maximum provided that:
AG, PRB 82, 184504 (2010)

$$c_x = \varepsilon_\theta^{1/2}, \qquad c_y = \varepsilon_\theta^{-1/2}$$

$$\varepsilon_\theta = \cos^2\theta + \varepsilon\sin^2\theta$$

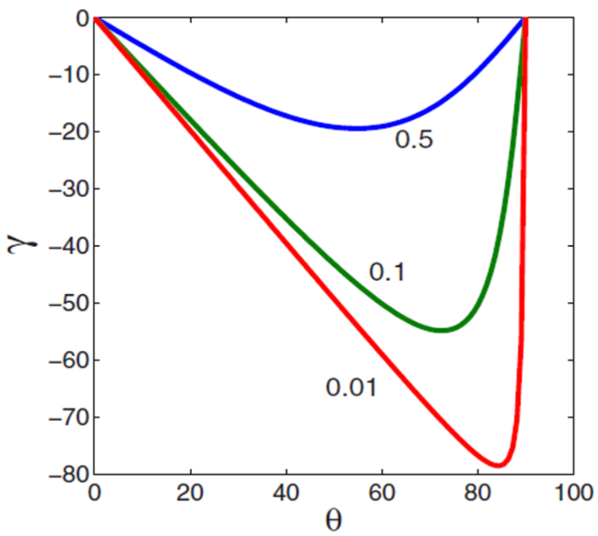

$$H_{c2}(\theta) = \frac{H_{c2}(0)}{(\cos^2\theta + \varepsilon\sin^2\theta)^{1/2}}$$

Equation for H_{c2} and Q

$$\ln t + U(t,b,q) = 0$$

$$U = 2e^{q^2}\,\mathrm{Re}\sum_{n=0}^{\infty}\int_0^{\infty} du\, e^{-u^2}\left\{\frac{u}{n+1/2} - \frac{t}{\sqrt{b}}\tan^{-1}\left[\frac{u\sqrt{b}}{(n+1/2)t + i\alpha b}\right]\right\},$$

$$b = \frac{\hbar^2 v^2 \varepsilon_\theta^{1/2} H}{8\pi\phi_0 T_c^2}, \qquad \alpha = \frac{4\mu_B \phi_0 T_c}{\hbar^2 v^2 \varepsilon_\theta^{1/2}}, \qquad q^2 = \frac{Q_z^2 \varepsilon \phi_0}{2\pi H \varepsilon_\theta^{3/2}}$$

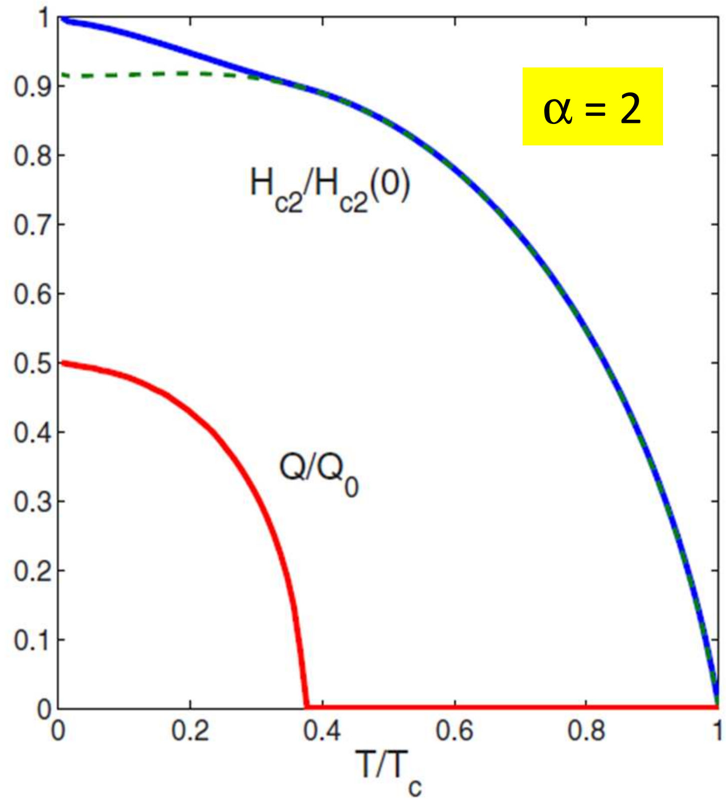

- FFLO transition for $\alpha > 1$
- Spontaneous FFLO vector Q(T) appears at low T
- The FFLO period $\ell(T) = 2\pi/Q(T)$ diverges at the spinodal: $T = T_{FFLO}$
- At zero T: $\ell(0) \sim \xi_0$. First order transition line between two spinodals.

Electron spectrum from ab-initio calculations and ARPES

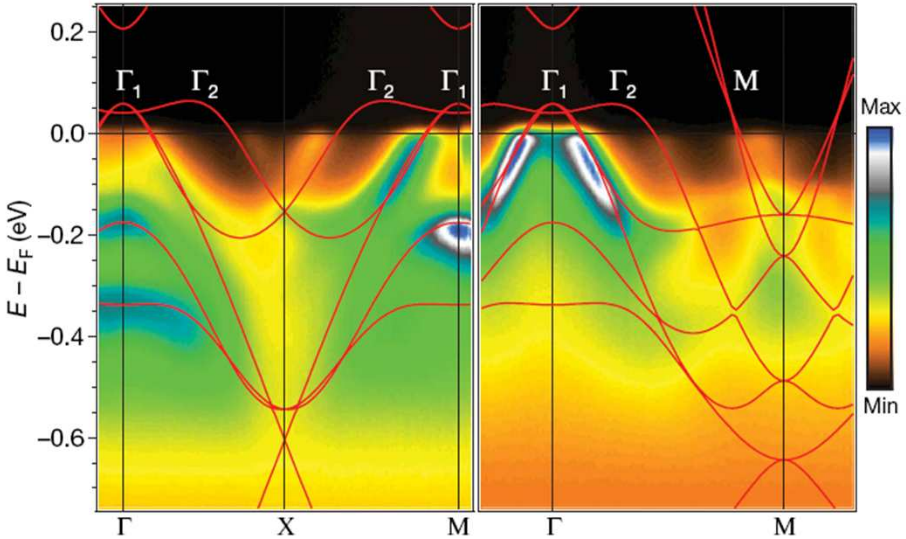

Figure 2 | Comparison between angle-resolved photoemission spectra and LDA band structures along two high-symmetry lines. ARPES data from LaOFeP (image plots) were recorded using 42.5-eV photons with an energy resolution of 16 meV and an angular resolution of 0.3°. For better

LaFeP(O,F)

- **multiple bands crossing the Fermi level**

two hole pockets at Γ and two electron pockets at M

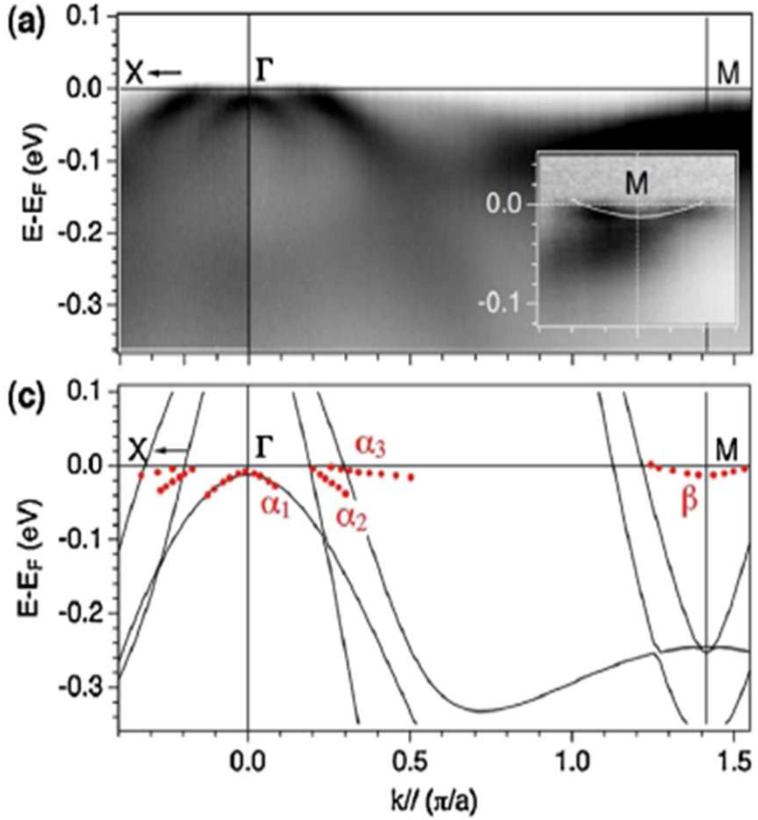

$FeSe_{0.42}Te_{0.58}$

Vol 455 | 4 September 2008 | doi:10.1038/nature07263 nature

LETTERS

Electronic structure of the iron-based superconductor LaOFeP

D. H. Lu[1], M. Yi[1], S.-K. Mo[1,2], A. S. Erickson[1], J. Analytis[1], J.-H. Chu[1], D. J. Singh[4], Z. Hussain[2], T. H. Geballe[1], I. R. Fisher[1] & Z.-X. Shen[1]

PRL 104, 097002 (2010) PHYSICAL REVIEW LETTERS week ending 5 MARCH 2010

Strong Electron Correlations in the Normal State of the Iron-Based $FeSe_{0.42}Te_{0.58}$ Superconductor Observed by Angle-Resolved Photoemission Spectroscopy

A. Tamai,[1] A. Y. Ganin,[2] E. Rozbicki,[1] J. Bacsa,[2] W. Meevasana,[1] P. D. C. King,[1] M. Caffio,[3] R. Schaub,[3] S. Margadonna,[4] K. Prassides,[5] M. J. Rosseinsky,[2] and F. Baumberger[1]

New features of FBS revealed by ARPES

- Small Fermi energies: **$E_F \sim$ 0.02-0.5 eV**

- Large effective mass renormalization:
  $m^* \sim (2\text{-}16) m_e$

- Several shadow bands near the FS:
  Lifshitz transition upon doping

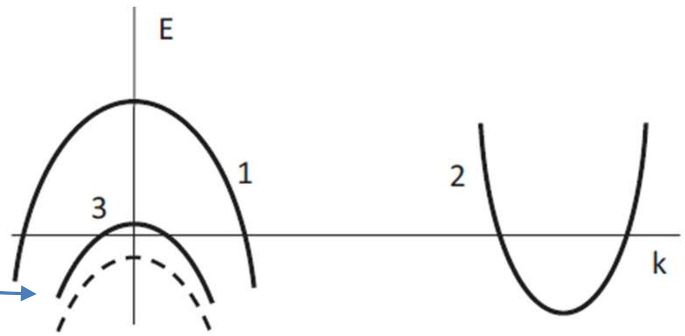

- Strongly correlated semimetals

- Good candidates for the FFLO state: $\alpha > 1$

- Example of a Pauli-limited SC: $FeSe_{0.5}Te_{0.5}$:
  T_c = 16K, E_F = 25 meV, $m_{ab} = 10 m_e$

$$\alpha = \frac{\pi k_B T_c m_{ab}}{E_F m_e}$$

α = 1.5 even for H||c

- In-plane coherence lengths $\xi \approx$ 1-2 nm

Multiband pairing gap symmetries

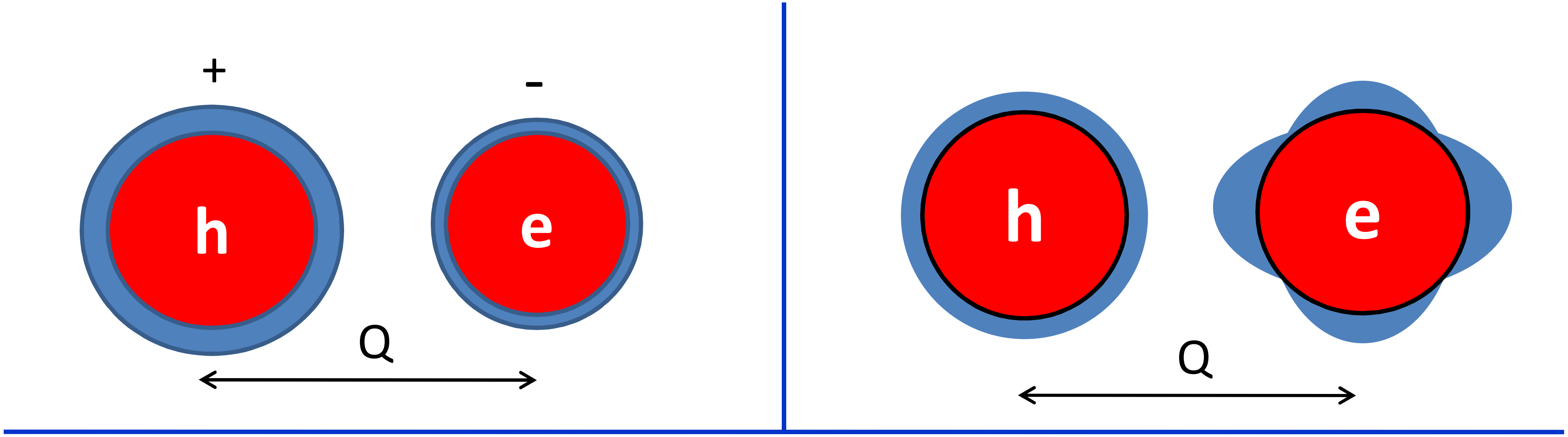

- $s^{\pm}$ pairing: gaps with opposite signs

Mazin, Singh, Johannes, Du, PRL 101, 057003 (2008);
Kuroki et al, PRL 101, 087004 (2008)

- Combined s and d-wave gaps

Kuroki et al, PRL 101, 087004 (2008);
Graser, Maier, Hirshfeld, Scalapino, NJP 11, 025016 (2009)

Strong interband repulsion: $\lambda_{12}\lambda_{21} > \lambda_{11}\lambda_{22}$

Phonons are not sufficient to explain high Tc

Pairing coupling constants

$$\Lambda = \begin{pmatrix} \lambda_{11} & \lambda_{12} \\ \lambda_{21} & \lambda_{22} \end{pmatrix}$$

Impurity scattering rates

$$\Gamma = \begin{pmatrix} \gamma_{11} & \gamma_{12} \\ \gamma_{21} & \gamma_{22} \end{pmatrix}$$

Critical temperature

Suhl, Mattias, Walker PRL 3, 552 (1959); Moskalenko, FMM 8, 25 (1959):

$$T_{c0} = 1.14\omega_D \exp[-(\lambda_+ - \lambda_0)/2w],$$

$$\lambda_\pm = \lambda_{11} \pm \lambda_{22}, \qquad \lambda_0 = \sqrt{\lambda_-^{\,2} + 4\lambda_{12}\lambda_{21}},$$

$$w = \lambda_{11}\lambda_{22} - \lambda_{12}\lambda_{21},$$

Interband coupling increases T_c

Pairbreaking interband impurity scattering

$$T_c \cong T_{c0} - \frac{\pi\gamma_{12}}{8}\left(1 \mp \sqrt{\frac{N_1}{N_2}}\right)^2$$

Golubov, Mazin, PRB 55, 15146 (1997);
AG, PRB 67, 184515 (2003)

- **Weak interband pairing** in MgB_2, $\lambda_{12}\lambda_{21} < \lambda_{11}\lambda_{22}$
- **Strong interband pairing** in pnictides, $\lambda_{12}\lambda_{21} > \lambda_{11}\lambda_{22}$

T_c suppression by impurities is much weaker for the two-gap s^{++}(-) than for $s^{\pm}$ (+)

Two-gap superconductivity in MgB_2

Big gap, $\Delta_\sigma \approx 7$ meV

Small gap, $\Delta_\pi = 2.3$meV

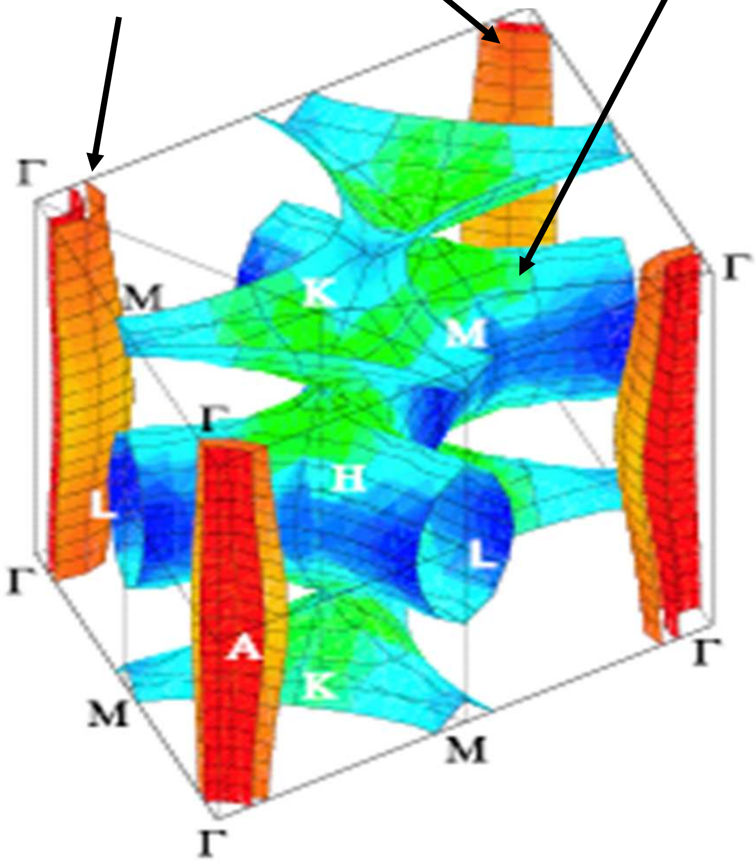

Liu, Mazin and Kortus (2002); Choi et al, (2002)

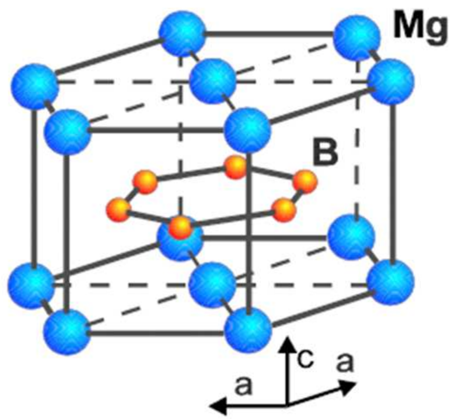

- 2D big gap for in-plane σ-orbitals s and 3D small gap for out-of-plane π-orbitals

- Weak interband coupling due to orthogonal p_z and p_{xy} orbitals of B

Band structure calculations:

$\lambda_{11} \approx 0.81$, $\lambda_{22} \approx 0.3$, $\lambda_{12} \approx 0.12$, $\lambda_{21} \approx 0.09$

$w = \lambda_{11}\lambda_{22} - \lambda_{12}\lambda_{21} > 0$

Multiband superconductivity on repulsion

- BCS gap equations for two bands:

$$\Delta_1 = \lambda_{11}\Delta_1 \int \frac{d\varepsilon}{E_1} \tanh\left(\frac{E_1}{2T}\right) + \lambda_{12}\Delta_2 \int \frac{d\varepsilon}{E_2} \tanh\left(\frac{E_2}{2T}\right)$$

where $E = (\varepsilon^2 + \Delta^2)^{1/2}$

$$\Delta_2 = \lambda_{22}\Delta_2 \int \frac{d\varepsilon}{E_2} \tanh\left(\frac{E_2}{2T}\right) + \lambda_{21}\Delta_1 \int \frac{d\varepsilon}{E_1} \tanh\left(\frac{E_1}{2T}\right)$$

- $s^{\pm}$ pairing for repulsive interaction $\lambda_{12} < 0$ and <u>opposite signs</u> of Δ_1 and Δ_2

- Pairing glue due to AF spin fluctuations, **$w = \lambda_{11}\lambda_{22} - \lambda_{12}\lambda_{21} < 0$**

$$\lambda_{nm} = \frac{JN_n\chi(Q)}{1 - JN_n\chi(Q)}$$

Convex H_{c2}(T) in two-band models

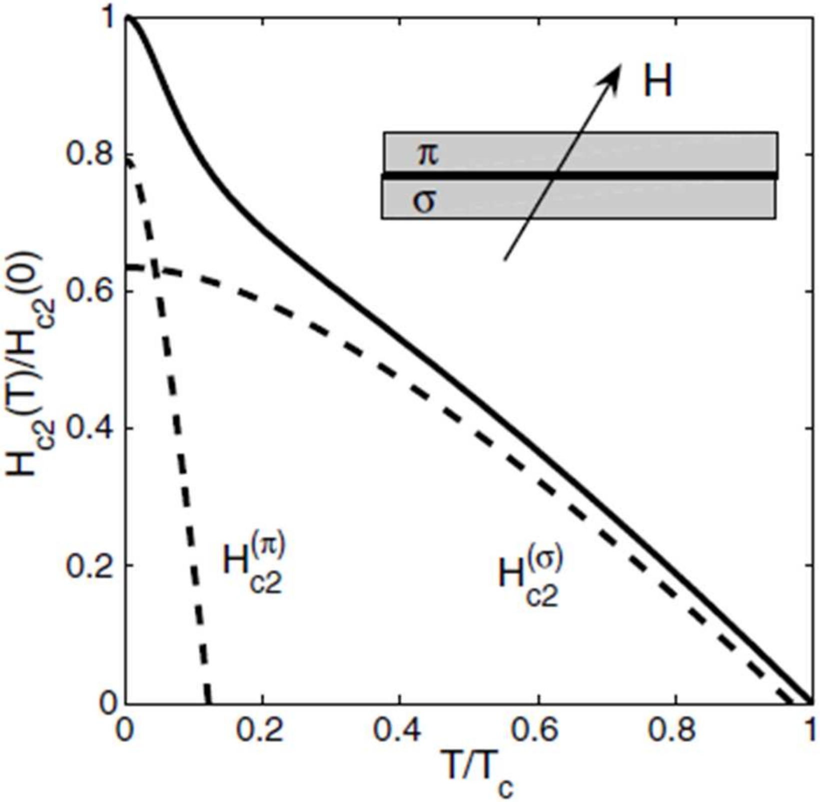

- Bilayer toy model of two-band SC
- Interaction of two bands with conventional H_{c2}(T) can produce unconventional H_{c2}(T) with upward curvature
- Model independent mechanism

H_{c2} for two coupled bands (clean limit) H||c

AG, PRB 82, 184504 (2010)
Rep. Prog. Phys. 74, 124501 (2011)

$$a_1(\ln t + U_1) + a_2(\ln t + U_2) + (\ln t + U_1)(\ln t + U_2) = 0,$$

$$U_1 = 2e^{q^2}\,\mathrm{Re}\sum_{n=0}^{\infty}\int_q^{\infty} du\, e^{-u^2}\left\{\frac{u}{n+1/2} - \frac{t}{\sqrt{b}}\tan^{-1}\left[\frac{u\sqrt{b}}{(n+1/2)t + i\alpha b}\right]\right\},$$

$$U_2 = 2e^{sq^2}\,\mathrm{Re}\sum_{n=0}^{\infty}\int_{q\sqrt{s}}^{\infty} du\, e^{-u^2}\left\{\frac{u}{n+1/2} - \frac{t}{\sqrt{b\eta}}\tan^{-1}\left[\frac{u\sqrt{b\eta}}{(n+1/2)t + i\alpha b}\right]\right\}$$

Band coupling parameters:

$a_1 = (\lambda_0 + \lambda_-)/2w$, $a_2 = (\lambda_0 - \lambda_-)/2w$, $\lambda_- = \lambda_{11} - \lambda_{22}$, $\lambda_0 = (\lambda_-^2 + 4\lambda_{12}\lambda_{21})^{1/2}$, $w = \lambda_{11}\lambda_{22} - \lambda_{12}\lambda_{21}$

Band asymmetry parameters:

$$\eta = \left(\frac{v_2}{v_1}\right)^2, \qquad s = \frac{\varepsilon_2}{\varepsilon_1}$$

Limiting cases for $\alpha << 1$

$$H_{c2}(T) = \frac{24\pi\phi_0 T_c(T_c - T)}{7\zeta(3)\hbar^2(c_+ v_1^2 + c_- v_2^2)}$$

$T \approx T_c$

- In the GL region, H_{c2} is limited by the FS pocket with the largest Fermi velocity. The s^{++} and $s^{\pm}$ scenarios behave similarly

$$H_{c2}(0) = \frac{\pi e^2 \phi_0 T_c^2}{2\gamma\hbar^2 v_1 v_2}\exp(g)$$

$$g = \left[\frac{\lambda_0^2}{w^2} + \frac{\lambda_-}{w}\ln(\eta) + \frac{ln^2\eta}{4}\right]^{\frac{1}{2}} sgn(w) - \frac{\lambda_0}{w}$$

- $H_{c2}(0)$ is limited by the largest Fermi velocity for the $s^{\pm}$ pairing but the smallest Fermi velocity for the s^{++} pairing

Can $s^{\pm}$ be distinguished from s^{++} ?

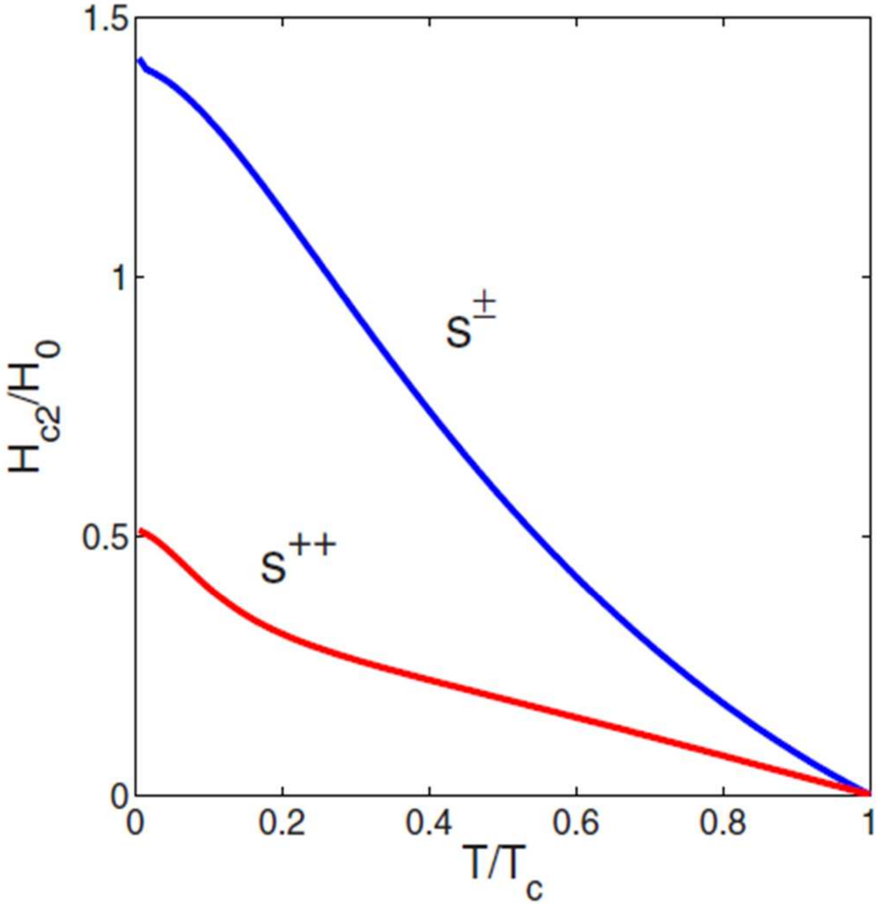

FIG. 5. (Color online) Comparison of $H_{c2}(T)$ curves for $s^{\pm}$ and s^{++} pairings and $\alpha=0$, where $H_0=8\pi\phi_0 k_B^2 T_c^2/\hbar^2 v_1^2$. The $s^{\pm}$ case was calculated for $\lambda_{12}\lambda_{21}=0.25$ and $\eta=0.01$. The s^{++} case was calculated for $\eta=0.01$ and λ_{lm} of MgB_2: $\lambda_{11}=0.81$, $\lambda_{22}=0.29$, $\lambda_{12}=0.13$, and $\lambda_{21}=0.09$ taken from Ref. 75.

No paramagnetic effects, $\alpha \ll 1$:

Strong band asymmetry causes upward curvature in $H_{c2}(T)$

Conventional s^{++} for MgB_2 : w > 0: convex $H_{c2}(T)$ at low T

Unconventional $s^{\pm}$ for pnictides : w < 0: convex $H_{c2}(T)$ at intermediate T

$s^{\pm}$ increases orbitally-limited H_{c2}

Mass anisotropy facilitates FFLO

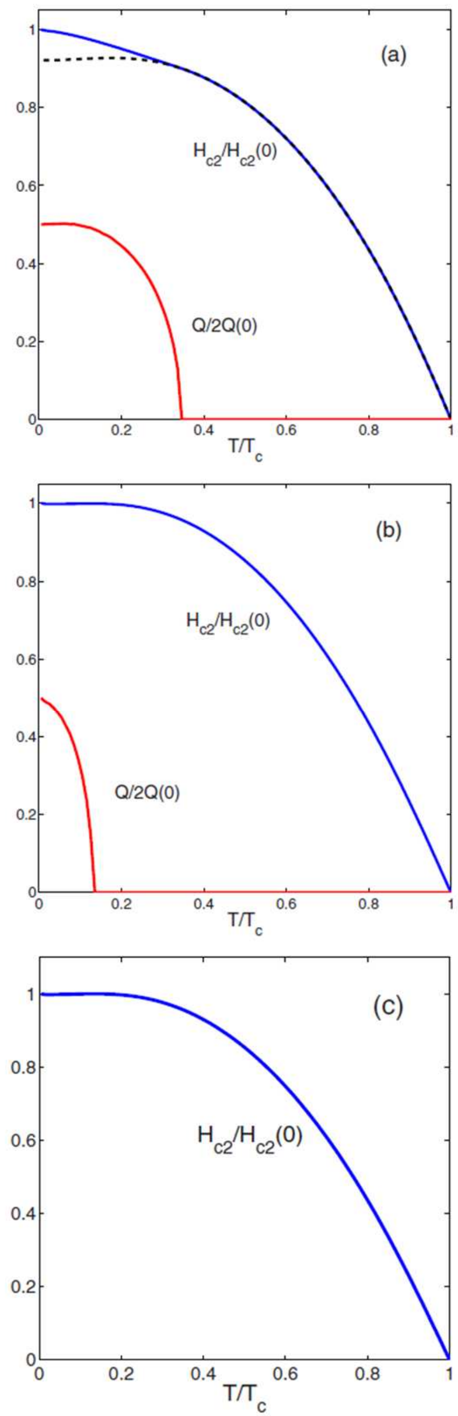

s = 0.01

s = 0.5

s = 1

η = 0.1

$$\eta = \left(\frac{v_2}{v_1}\right)^2, \qquad s = \frac{\varepsilon_2}{\varepsilon_1}$$

- If the passive band with $\alpha < 1$ has large mass anisotropy, the active band with $\alpha > 1$ can enforce the global FFLO state
- Reduction of the FFLO kinetic energy $\varepsilon_2 Q_z^2$ in the passive band 2 with $\alpha_2 < 1$.

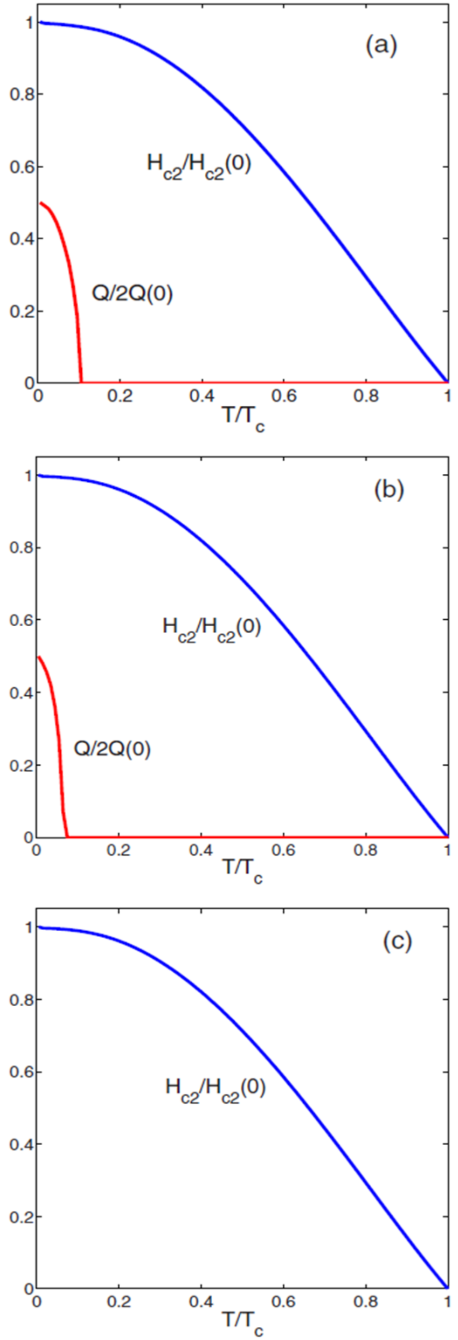

Band competition: hidden FFLO

$$\alpha_1 = \frac{2\pi k_B T_c}{v_1^2 m_e}, \qquad \alpha_2 = \frac{2\pi k_B T_c}{v_2^2 m_e}$$

- Due to the significant differences in the band parameters, one band can be FFLO unstable ($\alpha_1 > \alpha_c$) but another one is not ($\alpha_2 < \alpha_c$).
- Passive band reduces manifestations of the FFLO in the WHH-like shape of $H_{c2}(T)$, but FFLO is still there
- "Hidden" FFLO: no apparent signs in $H_{c2}(T)$ but can be revealed as the first order PT by magnetic torque and specific heat or NMR

Experiment-I: LiFeAs

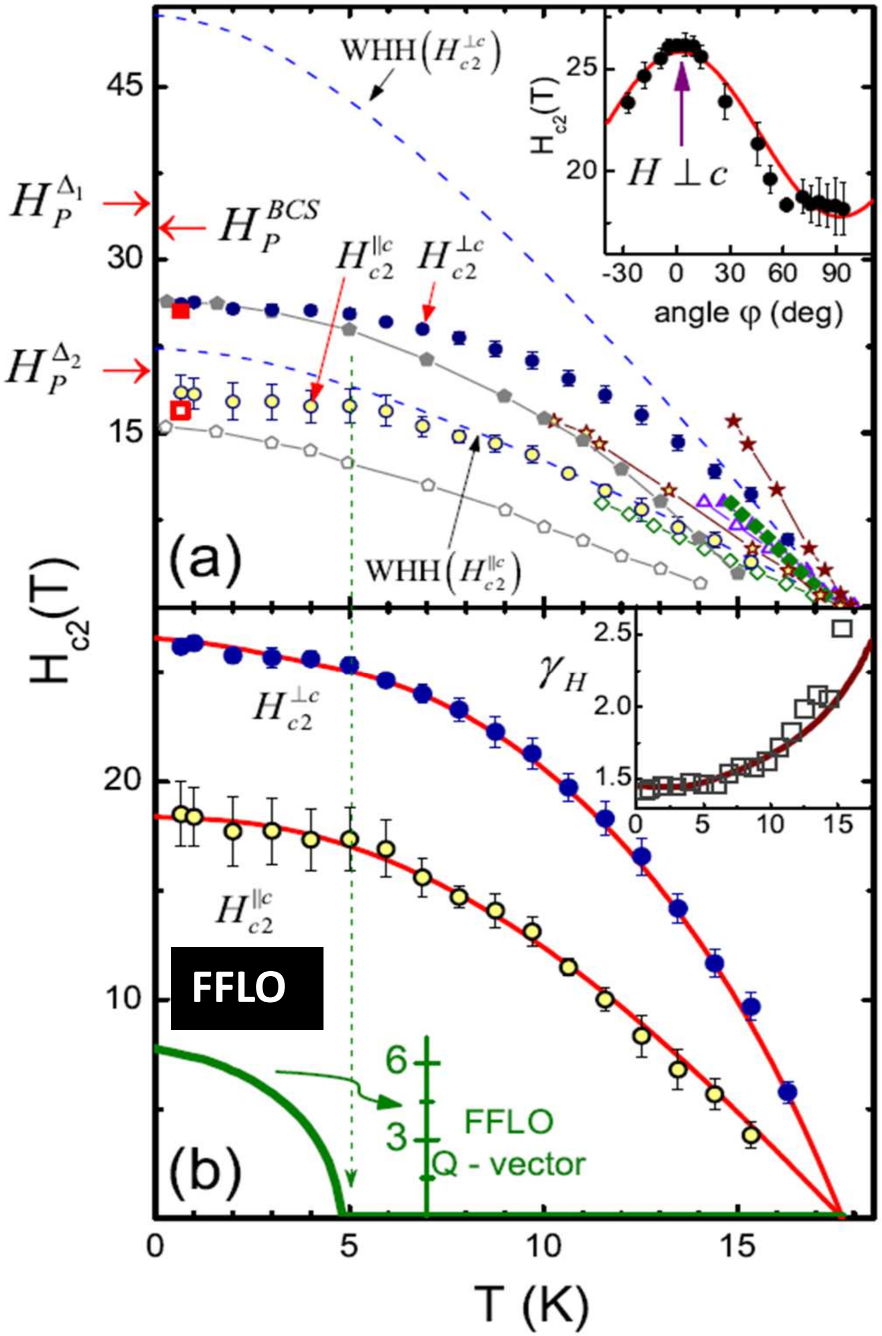

- Undoped composition corresponds to the maximum T_c
- No suppression of FFLO by doping - induced disorder
- Good candidate to search for FFLO, mean free path >> ξ

K. Cho, H. Kim, M. A. Tanatar, Y. J. Song, Y. S. Kwon, W. A. Coniglio, C. C. Agosta, AG, R. Prozorov, PRB, 83, 060502(R) (2011)

- Small jump in magnetic torque develops below 8K

N. Kurita et al. J. Phys. Soc. Jpn. 80, 013706 (2011)

Experiment-II: $FeSe_{0.5}Te_{0.5}$ films

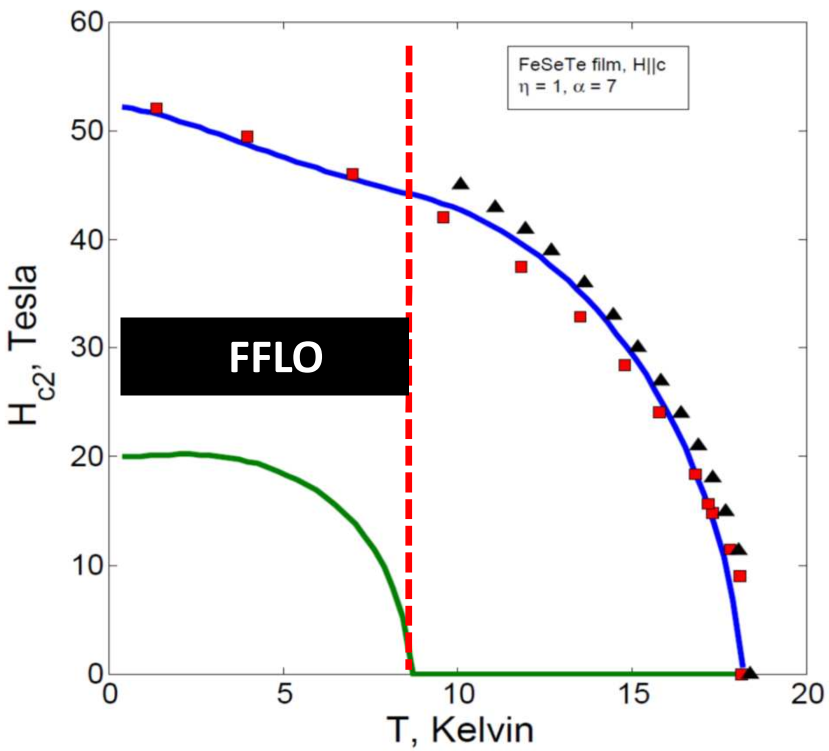

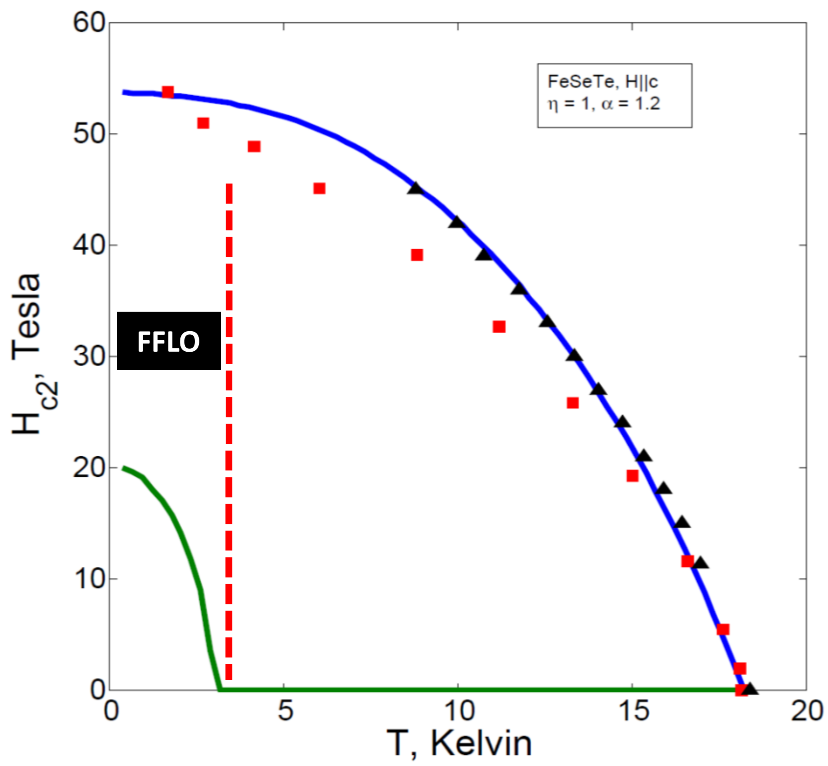

- 100-400 nm thick FeSeTe films, T_c = 16.2K. Huge slopes H_{c2}' > 100 T/K for H||ab

C. Tarantini et al. cond-mat. arXiv: 1108.5194

FFLO triggered by the Lifshitz transition

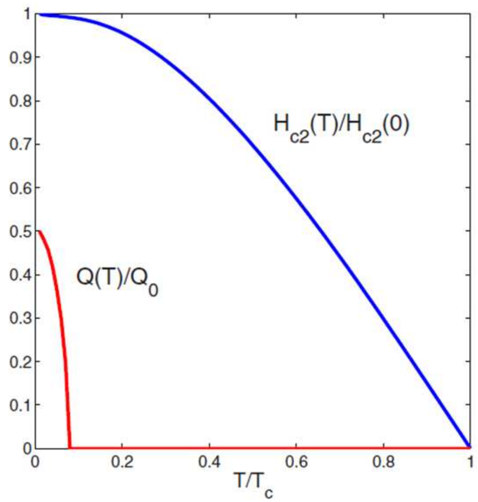

FIG. 9. (Color online) $H_{c2}(T)$ and $Q(T)$ calculated from Eq. (37) for $\alpha=0.3$, $\lambda=0.5$, $g=0.2$, $s=50$, $\eta=0.04$, and $Q_0=2Q(0)$.

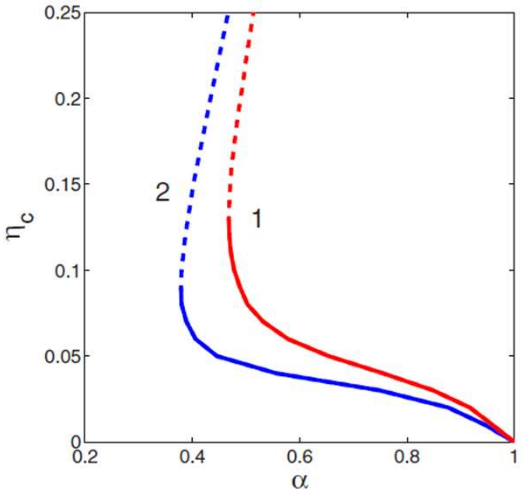

FIG. 10. (Color online) The critical value η_c calculated from Eqs. (41) for $m_3=2m_1$ and $s=25$ (1) and $s=10$ (2). The dashed curves show unstable branches of $\eta_c(\alpha)$.

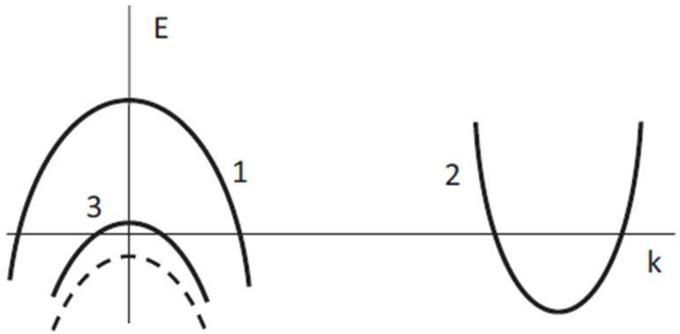

- H_{c2} equation in effective 2-band form:

$$\lambda(\ln t+\tilde{U}_1)(\ln t+U_2)=2\ln t+\tilde{U}_1+U_2,$$

$$\tilde{U}_1=\frac{U_1+gU_3}{1+g}, \qquad g=\frac{\lambda_{23}\lambda_{32}}{\lambda_{12}\lambda_{21}}=\frac{m_3^2V_{23}^2}{m_1^2V_{12}^2}\sqrt{\frac{\eta}{s}},$$

$$\lambda = (\lambda_{12}\lambda_{21} + \lambda_{23}\lambda_{32})^{1/2}$$

- reduction of the FFLO instability threshold

Enhancement factors

$$g = \frac{\lambda_{23}\lambda_{32}}{\lambda_{12}\lambda_{21}} = \frac{m_3^2 V_{23}^2}{m_1^2 V_{12}^2}\sqrt{\frac{\eta}{s}},$$

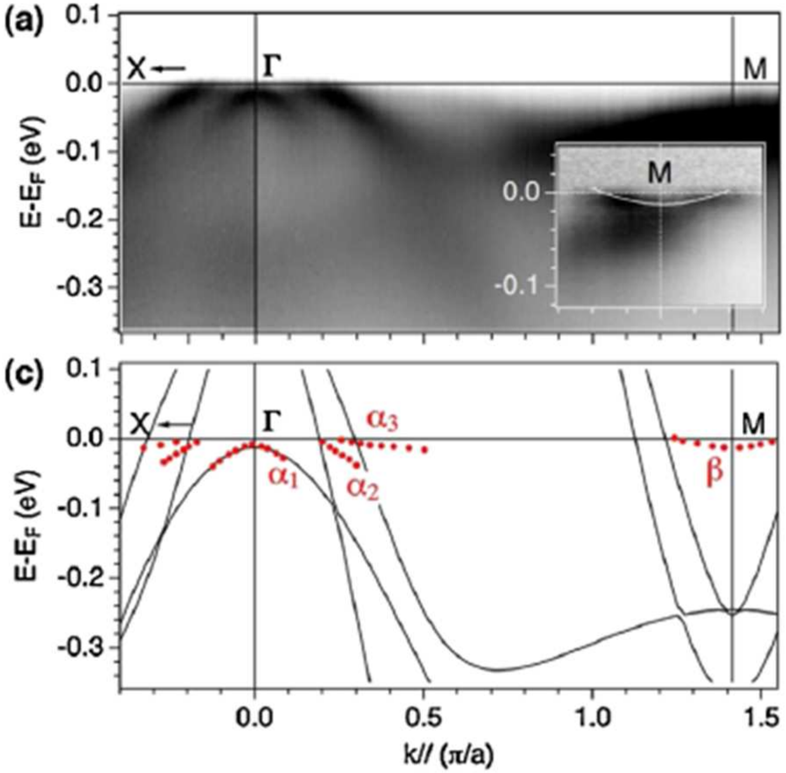

Small Fermi energies in FeSeTe

Tamai et al, PRL 104, 097002 (2010)

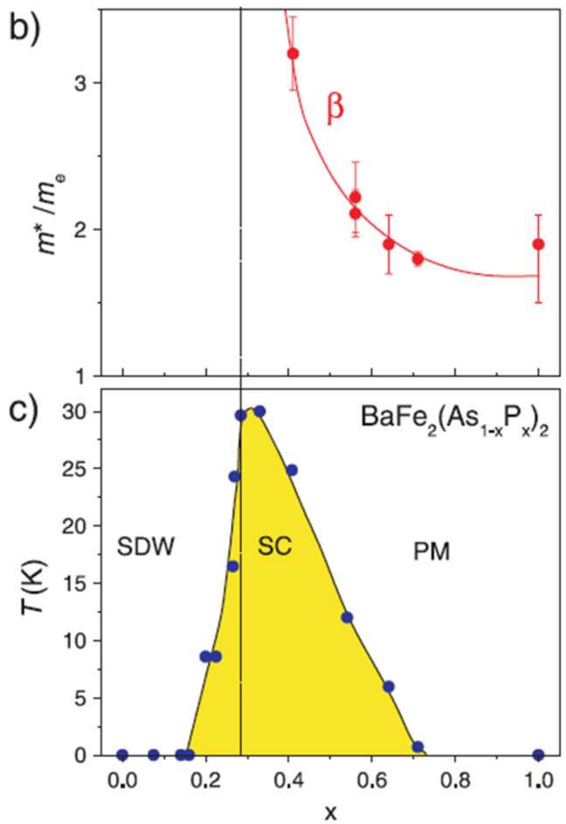

Mass enhancement of a shrinking FS Pocket $BaFe_2(As_xP_{1-x})_2$ revealed by dHvA oscillations

Shishido et al, PRL 104, 057008 (2010)

Quantum oscillations in $H_{c2}(T)$

- First LL quasiclassic solution works for $\alpha < 7$.
- For higher α (small E_F of the emerging FS pocket), quantum oscillations due to higher LLs become important

$$T_c(H) = T_{c0}(H)\left[1 - \sqrt{\frac{2\omega_c}{E_F}}\exp\left(-\frac{2\pi^2 T_{c0}}{\omega_c}\right)\sin\left(\frac{2\pi E_F}{\omega_c} + \frac{\pi}{4}\right)\right]$$

Rajagopal and Vasudevan, Phys. Lett. 23, 539 (1966)

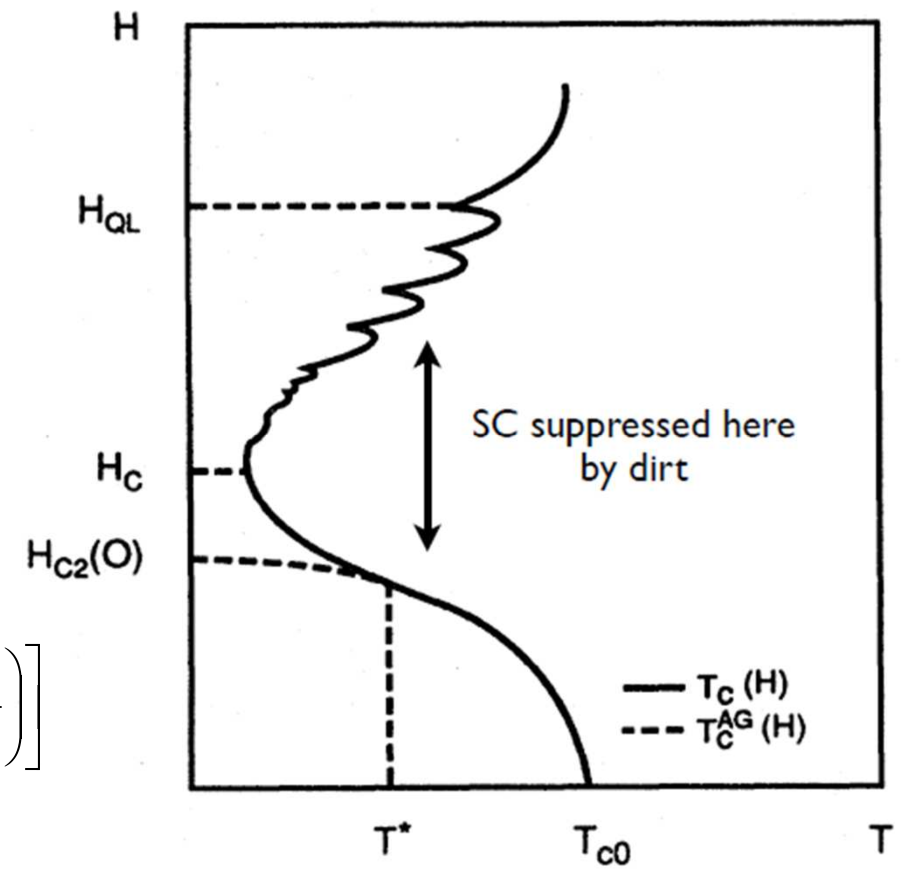

For a single band, see, e.g.
Rasolt and Tesanovic, RMP, 64, 709 (1992)

For E_F = 3 meV, the field range H ~ 30T is accessible at low temperatures

Magnetic defects caused by α particle irradiation

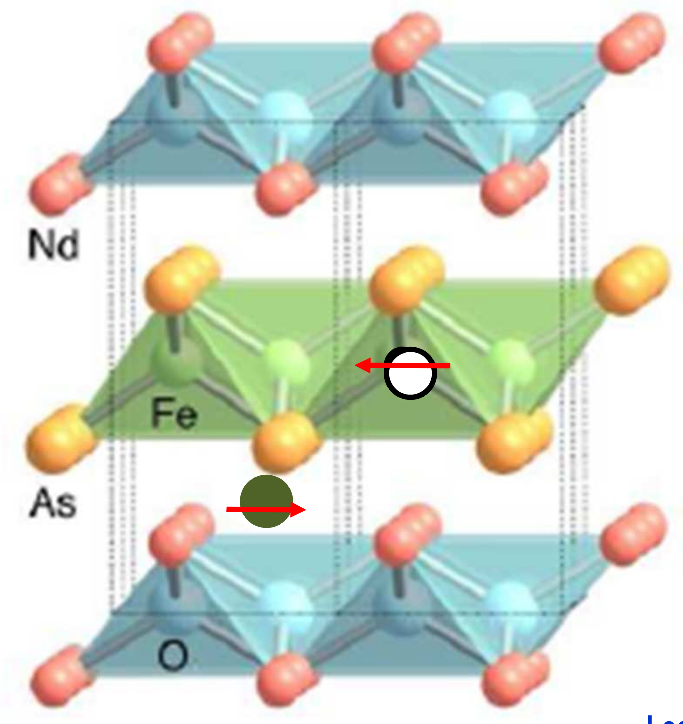

- A "clean" way of introducing disorder without doping and segregation of impurity phases
- α particles mostly interact with Nd, As and Fe.
- Displacement of Fe produces the Frenkel radiation defects
- Partial restoration of magnetic moment of Fe^{2+} ion
- Irradiation defects cause both nonmagnetic and magnetic scattering

Lee, Prado and Pickett, PRB 78, 174502 (2008)
Kemper et al, PRB 80, 104511 (2009)

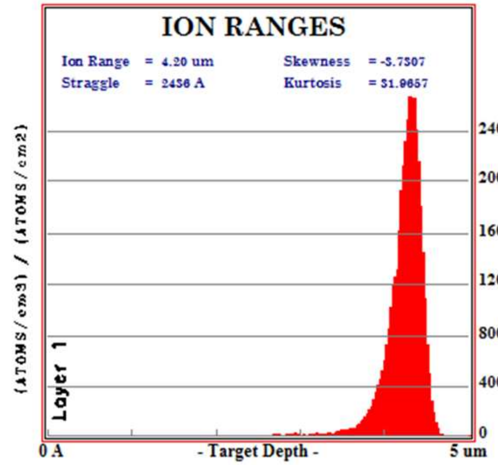

2 MeV $^4He^{2+}$ ion beam

Ion range in $NdFeAsO_{0.7}F_{0.3}$ ~ 4.2 μm
Uniform damage across the 1 μm thick crystal

Effect of irradiation on ρ(T) of a Nd-1111 single crystal

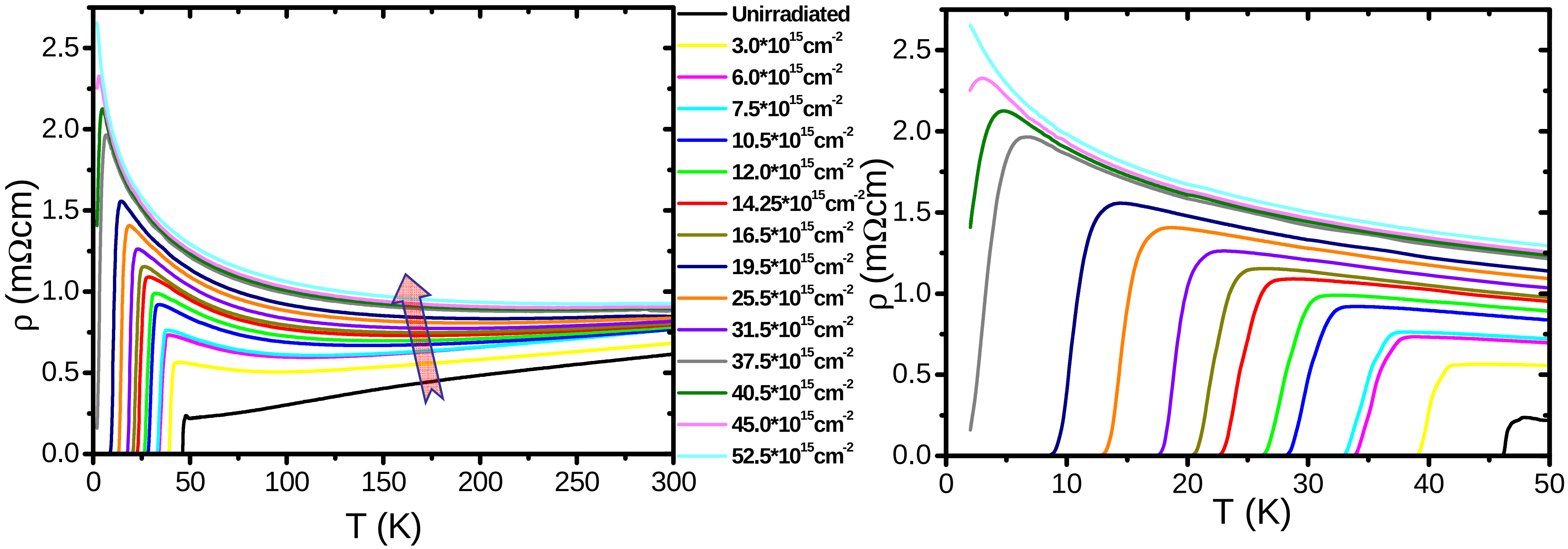

- T_c gradually decreases and the resistivity increases after each irradiation dose with a significant upturn developing at low T

- T_c vanishes at a rather high dose = 5.25×10^{16} cm^{-2}.

C. Tarantini , M. Putti, AG *et al. PRL* 104, 087002 (2010)

Logarithmic resistivity

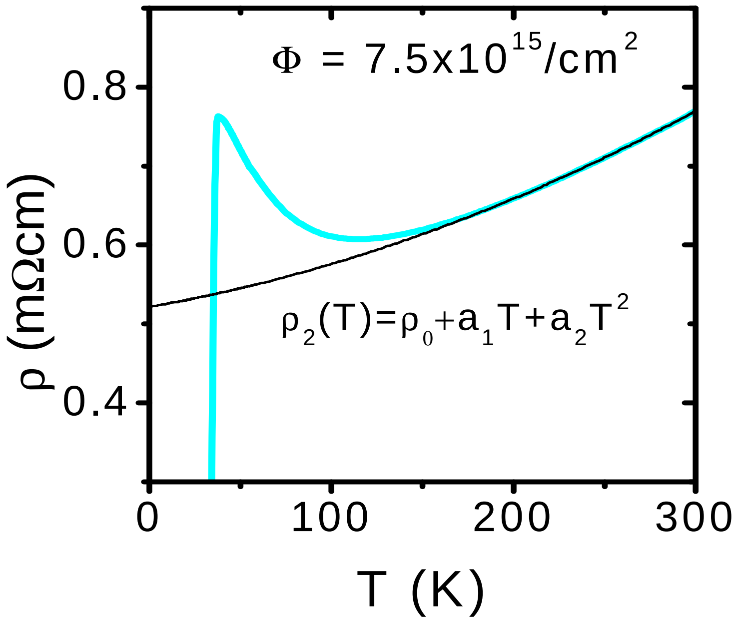

$$\rho_2(T) = \rho_0 + a_1 T + a_2 T^2$$

$$\Delta\rho(T) = \rho(T) - \rho_2(T)$$

- Logarithmic temperature dependence

$$\Delta\rho(T) = A_K \ln(T_0 / T)$$

- A_K increases with fluence
- $T_0 \approx$ 110-120 K is independent of fluence

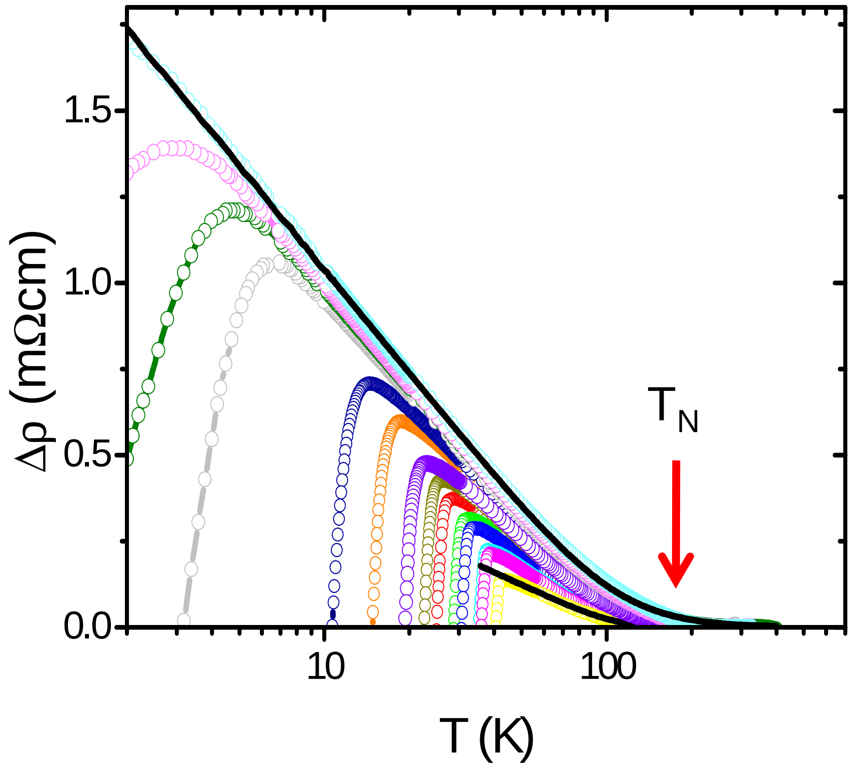

- Kondo scattering induced by irradiation?
- No sign of saturation at low T.
  Kondo temperature T_K < 2K

Dependence of fluence

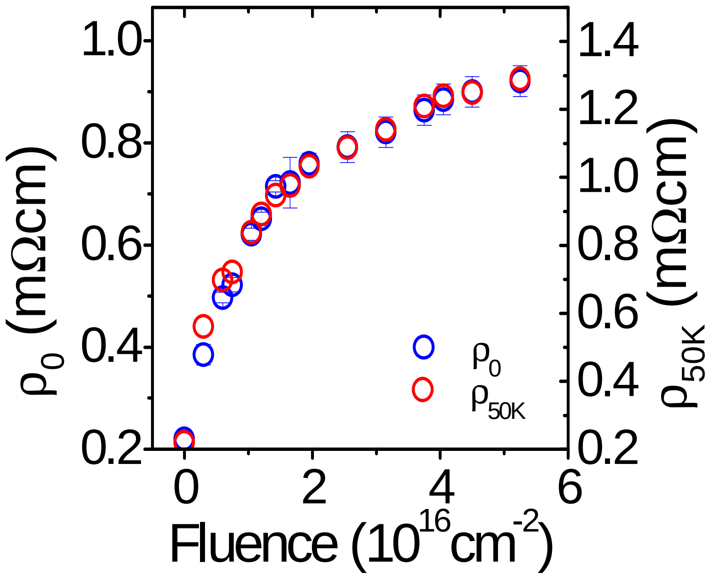

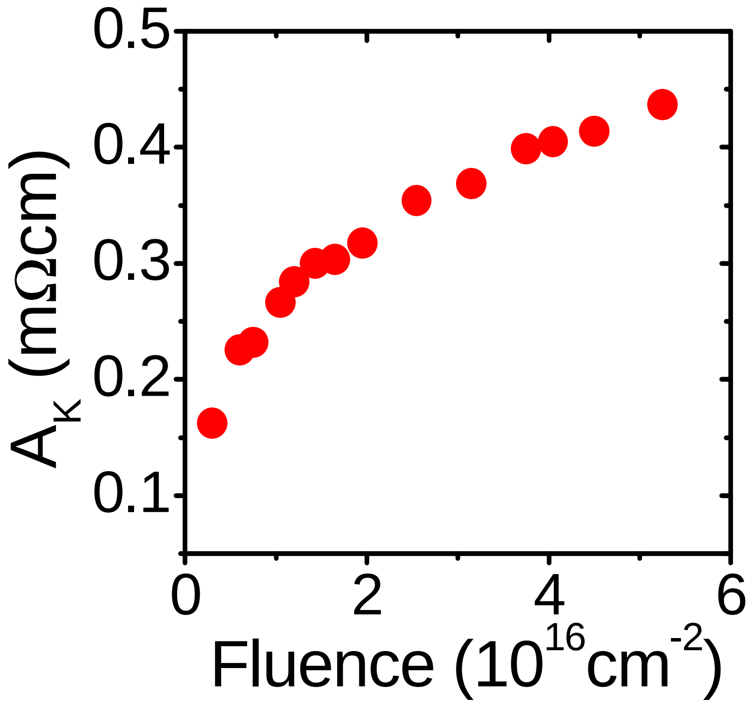

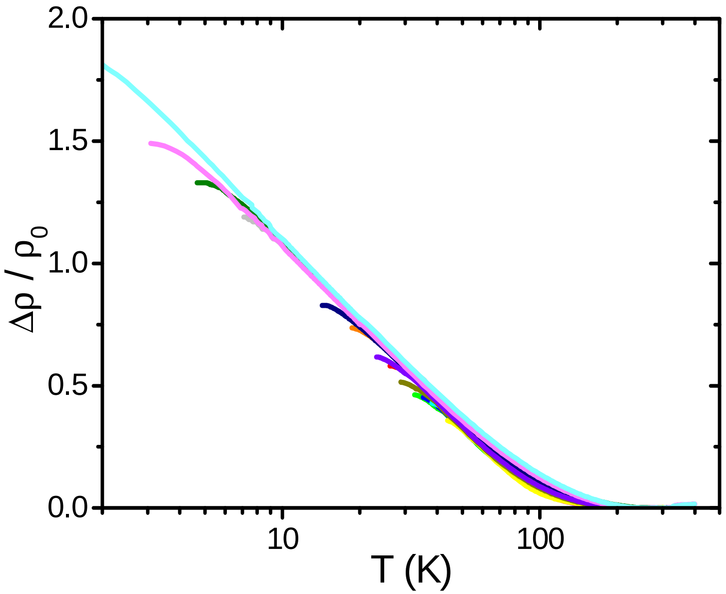

ρ_0 and A_K quantify non-magnetic and magnetic scattering

Both $\Delta\rho$ (T) and ρ_0 have the same dependence on the concentration of the irradiation defects

Suppression of T_c by irradiation defects

Non-magnetic scattering rate Γ

$$\Gamma = \Delta\rho_0 / \mu_0 \lambda_0^2$$

Pairbreaking interband scattering rate g

$$g = \Gamma\hbar / 4\pi k_B T_{c0}$$

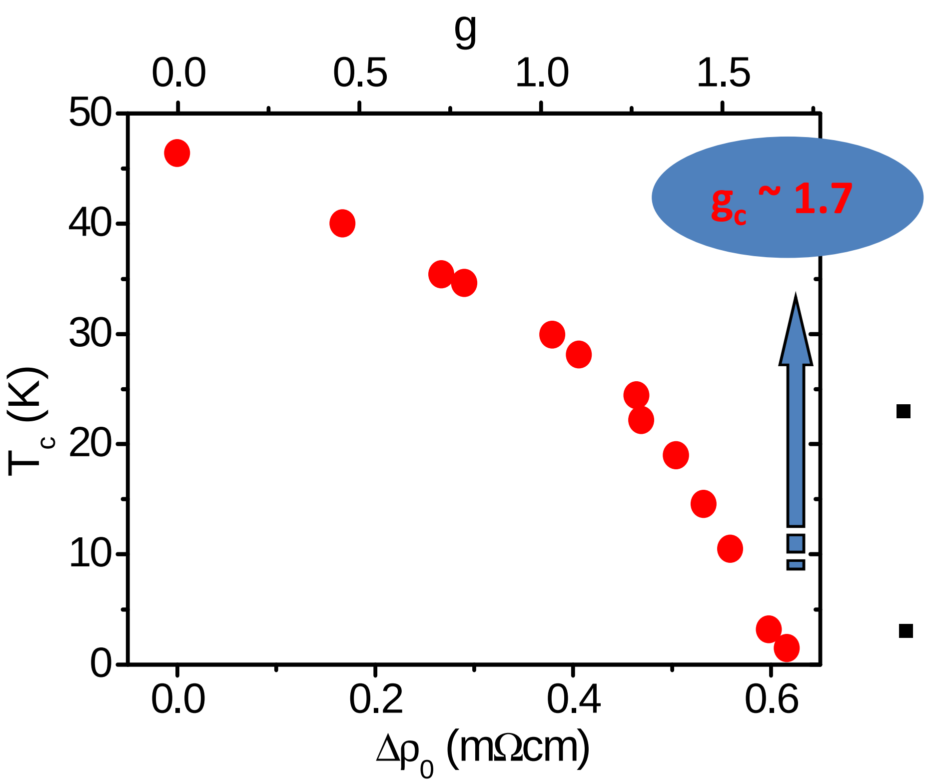

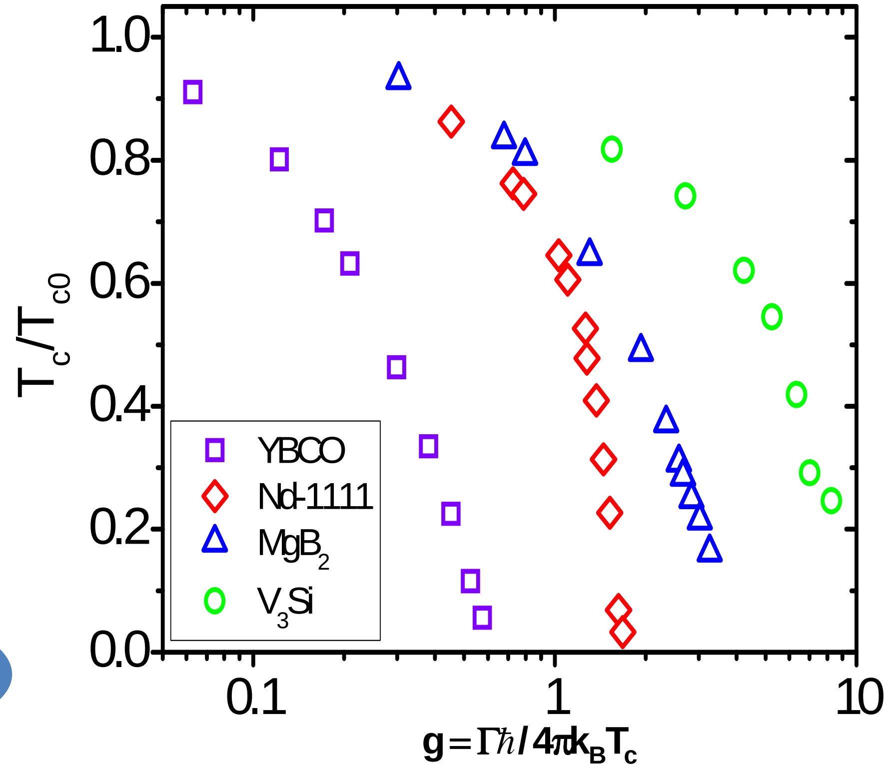

- **Nd-1111 looks more like the s-wave MgB_2 and V_3Si rather than the d-wave cuprates**
- **High density of irradiation defects: mean free path $l = v_F/\Gamma$ ~ 2.4nm**

Effect of scattering on T_c

Equal gaps: $\Delta_1 = -\Delta_2$:

Pairbreaking:
- Nonmagnetic inter-band scattering
- Magnetic intra-band scattering

Non-pairbreaking:
- Intra-band nonmagnetic scattering
- Inter-band magnetic scattering

Reduction of nonmagnetic inter-band scattering for strong impurity potentials

$$\frac{1}{2\tau} \rightarrow \frac{\pi c N V^2}{1+(\pi N V)^2}$$

G. Priosti and P. Muzikar, PRB 54, 3489 (1996);
M. Kulic and O. Dolgov, PRB 60, 13062 (1999).

$s^{\pm}$ two-band pairing

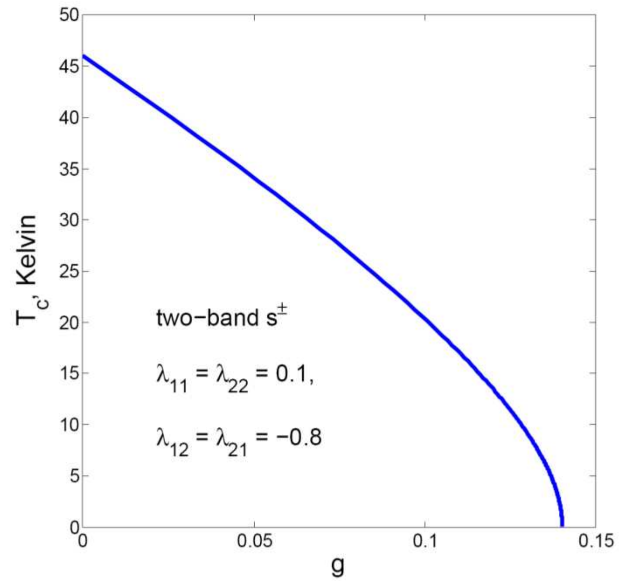

$g_c = 1/4\pi T_c\tau \approx 0.15$

Irradiation experiment gives $g_c \approx 1.7$

Magnetic Kondo scattering

- **Strong intra-band Abrikosov-Gorkov magnetic pairbreaking**

$$\ln\frac{T_{c0}}{T_c} = \psi\left(\frac{1}{2}+\frac{1}{4\pi\tau_s T_c}\right)-\psi\left(\frac{1}{2}\right)$$

- **Effect of Kondo scattering on BCS superconductivity:**

E. Muller-Hartmann, J. Zittartz, PRL 26, 428 (1970); P. Schlottmann, SSC 21, 663 (1973);
T. Matsuura, S. Ichinose , Y. Nagaoka, Prog. Theor. Phys. 57, 713 (1977);
M. Jarrell, PRB 41, 4815 (R) (1990).

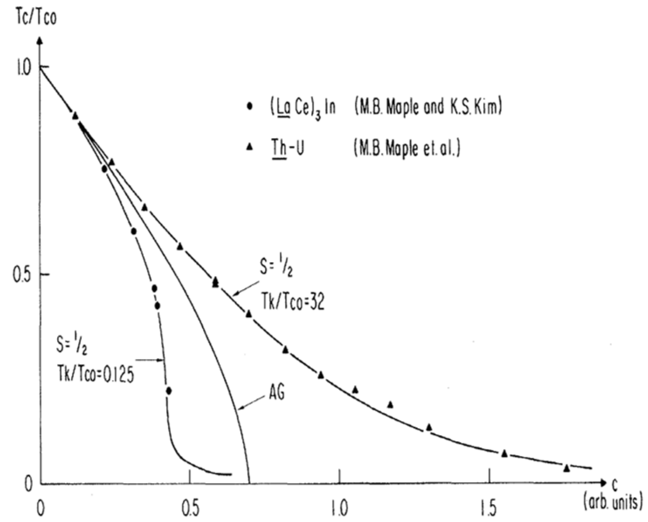

E. Muller-Hartmann, J. Zittartz, PRL 26, 428 (1970)

- **$T_K > T_{c0}$: Kondo screening reduces pairbreaking as compared to the AG theory**

- **$T_K < T_{c0}$: Kondo scattering enhances pairbreaking as compared to the AG theory. Multi-valued dependence of T_c on the impurity concentration**

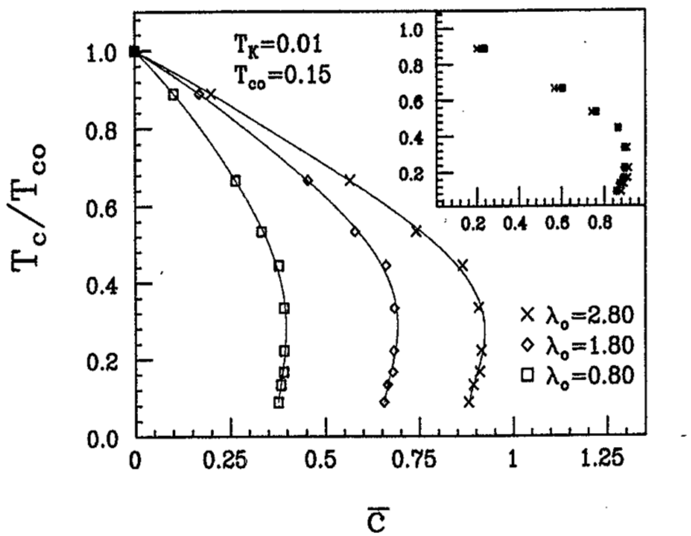

M. Jarrell, PRB 41, 4815(R) (1990).

For Nd-1111 crystals, T_K < 2K and T_c = 46K: any multiband BCS superconductivity would be suppressed irrespective of pairing symmetry

Conclusions

- Anomalous temperature depencencies of $H_{c2}(T)$ reflect the effects of multiband pairing and strong Pauli limiting in FBS

- $s^{\pm}$ pairing, low carrier density and high T_c enhance the orbitally-limited $H_{c2}(T)$

- Strong Pauli pairbreaking in FBS can lead to FFLO.

- Hidden FFLO in multiband FBS: The WHH shape of $H_{c2}(T)$ does not mean the absence of FFLO . Torque, NMR and specific heat experiments at high fields are needed.

- Possibility of tuning $H_{c2}(T)$ by doping but not disorder: FFLO triggered by the Lifshitz transition

- Unusual behavior of Kondo impurities in pnictides: strong enhancement of resistivity but weak suppression of T_c even for the mfp $\approx \xi$

- Magnetic impurity scattering is to be intertwined with pairing AF interaction

- Grossly enhanced paramagnetic limit: evidence for the AF enhancement of H_p